THE HIND LIMB ONTOGENY OF *TROODON FORMOSUS*

by

Harris Russell Boekenheide

A thesis submitted in partial fulfillment

of the requirements for the degree

of

Master of Science

in

Earth Sciences

MONTANA STATE UNIVERSITY

Bozeman, Montana

June 2023

ACKNOWLEDGEMENTS

I would like to thank my graduate advisor, Dr. David Varricchio, for his guidance and continued patience over the past four years. I don't know where I would be without you; the other members of my graduate committee, Dr. Matthew Carrano and Dr. John Scannella for always being willing to provide their expertise when asked; Don and Penni Collins of Montana Emu Ranch Co. for the generous donation of emus; Eric Metz for instruction on modern bone preparation; Ellen Lamm for instruction on thin section imaging; Dr. Michael D'Emic for advance notice on the tibia-femur circumference equation; Dr. Holly Woodward for histology imaging advice; my graduate cohort for being such an effective escape from work; to Heath Caldwell and Emilio Bedolla for taking over emu duty and putting an end to the complaints about the smell in the CVA lab; to Mike for always patiently enduring the nonsense I say; to Museum of the Rockies for the loan of Troodon specimens; the Blackfeet Nation, the families of Lewis Carroll, Vernon Carroll, Huey Monroe, MOR inc., The Nature Conservancy, and the Peebles families for permission to excavate and collect the fossils from their land; the National Science Foundation for funding John Horner's field work when these specimens were collected; and Montana State University's Department of Earth Sciences. Finally, I would like to thank my parents for their tireless support and understanding.

TABLE OF CONTENTS

TABLE OF CONTENTS CONTINUED

TABLE OF CONTENTS CONTINUED

LIST OF TABLES

Table Page

LIST OF FIGURES

Figure Page

LIST OF FIGURES CONTINUED

Figure Page

LIST OF EQUATIONS

Equation Page

ABSTRACT

The Campanian theropod *Troodon formosus* has long been recognized as one of the most exceptional dinosaurs of the Late Cretaceous. Despite its relatively small size, it was a remarkably advanced and specialized creature, with one of the largest encephalization quotients among dinosaurs, serrated teeth with hypertrophied denticles, and long hind limbs suited for agility and energy-efficient locomotion. Yet much is still unknown about members of this species due to the fragmentary and disassociated nature of what has thus far been uncovered. In the hopes of better understanding this species, we used the histology and bone scaling of the pelvic limbs of *Troodon* and the modern emu to make inferences about its ontogeny. This resulted in the discovery of highly variable growth strategies in *Troodon* individuals, as well as further evidence that modern cursorial avians are not an apt modern analogue for *Troodon* ontogeny and locomotion.

CHAPTER ONE

INTRODUCTION

Troodon

Troodon Biology

Troodon formosus is a small troodontid theropod from the Campanian of northern North America, known mostly from the Two Medicine, Dinosaur Park, Judith River, and Oldman Formations. *Troodon,* as its name (meaning "wounding tooth") suggests, is mainly believed to have been a predatory carnivore. This theropod lived in near-marine environments containing seasonal floodplains, though it has been suggested to have preferred more inland locales (Russell, 1969; Brinkman, 1990). *Troodon* was remarkably advanced even among Late-Cretaceous theropods; with large forward-facing orbits indicative of nocturnal predation; an enlarged middle ear for hearing; a hind limb morphology denoting a high degree of agility and balance; and proportionally one of the largest braincases found in non-avian theropods, indicative of a level of intelligence comparable to that of modern ratites (Makovicky & Norell, 2004).

Troodon Naming and Classification

The notoriously complex history of disputes regarding the species started in 1855, when Dr. Ferdinand Hayden found the holotype specimen, a lone tooth with unusually large denticles within the Judith River formation of what is now known as central Montana. The very next year, Joseph Leidy named the species *Troodon validus* and described it, concluding that the tooth belonged to a lizard.

Franz Nopcsa reassigned the tooth to Megalosauridae in 1901. In 1924, Charles Gilmore came to synonymize *Troodon* with *Stegoceras*, assigning them to a new family under the designation of "Troodontidae," which he described as a family of "thick-domed ornithischians." A foot was found in 1932 that would be attributed to a new genus, which would be named *Stenonychosaurus.* It was not until 1945, that Charles Mortram Sternberg placed the tooth back into Theropoda. In 1987, Currie concluded that *Stenonychosaurus* was a junior synonym for *Troodon.* Debates regarding *Troodon's* name and phylogenetic placement continue to this day (Zanno et al. 2011; Larson & Currie 2013; van der Reest & Currie 2017; Cullen et al., 2021), but will not be the subject of this paper.

Why Hind Limbs

Hind limbs can tell us a great deal about an organism, from body mass to locomotive capabilities. From those, we can make interpretations on overall size, growth rates, predation strategies, ecological niche, and much more. Its large EQ, highly serrated teeth, and trend toward greater degrees of cursoriality (Fowler et al., 2011) indicate that *Troodon* was intelligent, deadly, and incredibly mobile. This paper aims to gain a greater understanding of this taxon by examining its hind limbs through ontogeny, with a focus on growth rates and body mass, cursoriality, and allometry.

Literature Cited

Brinkman, D. B. (1990). Paleoecology of the Judith River Formation (Campanian) of Dinosaur Provincial Park, Alberta, Canada : evidence from vertebrate microfossil localities. Palaeogeography, palaeoclimatology, palaeoecology, 78(1-2), 37-54.

Cullen, T. M., Zanno, L., Larson, D. W., Todd, E., Currie, P. J., & Evans, D. C. (2021). Anatomical, morphometric, and stratigraphic analyses of theropod biodiversity in the Upper Cretaceous (Campanian) Dinosaur Park Formation. Canadian journal of earth sciences, 58(9), 870-884. https://doi.org/10.1139/cjes-2020-0145

Fowler, D. W., Woodward, H. N., Freedman, E. A., Larson, P. L., & Horner, J. R. (2011). Reanalysis of "Raptorex kriegsteini"; a juvenile tyrannosaurid dinosaur from Mongolia. PloS one, 2011(6), e21376-e21376. https://doi.org/10.1371/journal.pone.0021376

Makovicky, P. J., & Norell, M. A. (2004). Troodontidae. In D. B. Weishampel, P. Dodson, & H. Osmóska (Eds.), The Dinosauria (2 ed., pp. 184-195): University of California Press.

Russell, D. A. (1969). A new specimen of Stenonychosaurus from the Oldman Formation (Cretaceous) of Alberta. Canadian journal of earth sciences, 6(4), 595-612. https://doi.org/10.1139/e69-059

Varricchio, D. J. (1997). Troodontidae. In P. J. Currie & K. Padian (Eds.), The Encyclopedia of Dinosaurs (pp. 749-754). San Diego: Academic Press.

CHAPTER TWO

BODY SIZE AND GROWTH VARIATION IN *TROODON FORMOSUS* AS OBSERVED THROUGH LIMB HISTOLOGY

Contribution of Authors and Co-Authors

Manuscript in Chapter 2

Author: Harris R. Boekenheide

Contributions: Designed project and drafted manuscript, gathered and interpreted data, created figures.

Co-Author: David J. Varricchio

Contributions: Editing, provided direction, advice, expertise

Co-Author: Matthew T. Carrano

Contributions: Editing, provided advice and expertise

Manuscript Information

Harris R. Boekenheide, David J. Varricchio, Matthew T. Carrano

Journal of Vertebrate Paleontology

Status of Manuscript:

__x__ Prepared for submission to a peer-reviewed journal

____ Officially submitted to a peer-reviewed journal

____ Accepted by a peer-reviewed journal

____ Published in a peer-reviewed journal

Body size and growth variation in *Troodon formosus* as observed through limb histology

HARRIS R. BOEKENHEIDE[*,1], DAVID J. VARRICCHIO[2], MATTHEW T. CARRANO[3]

[1]Department of Earth Sciences, Montana State University, Bozeman, Montana 59717, U.S.A., hrboekenheide@gmail.com;

[2]Department of Earth Sciences, Montana State University, Bozeman, Montana, 59717, U.S.A., djv@montana.edu;

[3]Paleobiology Department, Smithsonian National Museum of Natural History, Washington, D.C., 20560, U.S.A., carranom@si.edu

*Corresponding author

Abstract

ABSTRACT— The Campanian troodontid theropod *Troodon formosus* has been the subject of paleontological study for over 150 years. However, our understanding of the species has been limited by a relative lack of articulated elements. The circumferences of hind limb bones, most notably the femur, have long been used to estimate the body mass of non-avian theropods, as they are the main weight-bearing bones of bipedal animals. Using annually deposited lines of arrested growth and other skeletal growth markers observed in histologic thin section, it is possible to track yearly increases in the body masses of fossil organisms. Using new body mass estimation methodologies, we document an increase in the adult body mass of *Troodon* and the presence of variable growth rates among individuals, which we attribute to sexually dimorphism.

INTRODUCTION

The Campanian troodontid theropod *Troodon formosus* has long been a subject of intrigue and debate. With the unusual tooth morphology that inspired its namesake, adaptations favoring relatively high degrees of cursoriality (Fowler et al., 2011; Persons & Currie, 2014), and a high encephalization quotient comparable to that of modern ratites (Makovicky & Norell, 2004), it was among the most exceptional theropods of its time. Through histologic examination of the hind limb bones, we hope to gain a better understanding of ontogenetic growth in this remarkable species.

Histologic Growth and Skeletal Growth Markers

Markers of growth can be found in all bone tissue types within the bones of all vertebrates (Buffrénil & Quilhac, 2021). Although variation may be present, these growth markers are very often cyclical in nature representing approximately one year of growth. Annual bone deposition is generally composed of three parts: a zone, followed by an annulus, and then a line of arrested growth (LAG). A “zone” is the area that represents the period each year in which growth is most rapid, and is typically represented by woven-fibered bone. “Annuli” are bands of poorly-vascularized bone comprised of more parallel-fibered bone in which growth is still occurring but has slowed down (Francillon-Vieillot et al., 1989; Castanet et al., 1993). The structural composition differentiating them from zones produce a subtle, yet noticeable change in the bone’s texture due to differences in fiber organization (Cerda et al., 2017). LAGs are ring-like structures made up of avascular, lamellar bone that are indicative of periods in which growth has significantly slowed or ceased entirely (Erickson, 2005).

As in one of Dinosauria's closest extant relatives, crocodilians, LAGs are generally considered to be annual markers formed during cyclical periods of decreased access to nutritional resources. (Castanet & Naulleau, 1985). LAGs are believed to be reliable representations of a fixed portion of time (approximately one year), as resource scarcity is often seasonal in nature. It should be noted that while annuli and LAGs are most often found together, LAGs can be found without a corresponding annulus, and vice versa (Buffrénil & Quilhac, 2021). An annulus found without an accompanying LAG may have been produced by seasonal irregularities, such as an unusually warm winter preventing the full formation of a LAG or an unusually cold summer resulting in slowed growth. Therefore, depending on the circumstances, unaccompanied annuli may or may not be indicators of annular growth. The presence of several closely-spaced LAGs toward the periosteal surface of a bone is known as an external fundamental system (EFS), a feature indicative of the cessation of growth and acquisition of somatic maturity (Padian & Lamm, 2013) [Fig. 2.1]

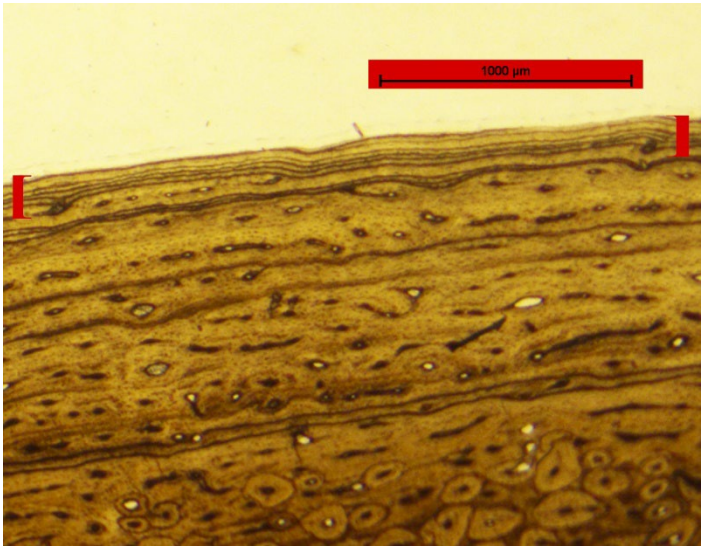

FIGURE 2. 1. MOR 553S-7.28.91.237, Example of an external fundamental system (EFS), denoted by brackets. The amount of new bone deposited between LAGs decelerates annually until bone growth has ceased entirely. [planned for column width]

METHODS

Institutional Abbreviations— **MOR**, Museum of the Rockies, Bozeman, U.S.A.

Anatomical Abbreviations— **EFS**, External Fundamental System; **LAG**, Line of Arrested Growth; **SGM**, Skeletal Growth Marker.

Geological Setting

Two Medicine Formation— All of the fossil specimens used for this study come from the Upper Cretaceous Two Medicine Formation of Montana. The Two Medicine Formation dates back to the late Campanian in age, between 82.419 +/- 0.074 Ma and 73.496 +/- 0.039 Ma (Ramezani et al., 2022). The Two Medicine Formation represents a transitionary zone between a subtropical environment and more temperate, semi-arid one, as evidenced by geologic, floral, and palynological data (Dodson, 1971; Crabtree, 1987; Wolfe & Upchurch, 1986; Krassilov, 1981; Jerzykiewicz & Sweet, 1987). MOR 553, MOR 563, and MOR 748 were all collected with permission from Blackfeet tribal lands.

Jack's Birthday Site— Jack's Birthday Site (MOR locality no. TM-068) is the location from which most of the fossils used in this study originate. First discovered in June of 1988, it is a multitaxon bonebed located near Badger Creek, within the Blackfeet Indian Reservation. The site represents the edge of what was once a shallow floodplain lake, transitioning from shoreline in the northwest to floodplain in the southeast, over the course of about 50m (Varricchio, 1995). Though predominantly iguanodontoid in composition, it contains dinosaurs from a total of ten different species, as well as several non-dinosaurian taxa, totaling over 1600 skeletal elements. It is also known as the first multi-individual occurrence of *Troodon*, with a minimum of six individuals. *Troodon* found at the site are highly disarticulated, and mainly concentrated at the

site's southern margin. Taphonomic studies of the site have determined the assemblage to likely be attritional and parautochthonous in nature (Varricchio, 1995).

Growth rates were determined by tracking annual increases in body mass. By measuring the circumferences of LAGs and annuli present in histological thin sections, it would be possible to estimate an individual's body mass year-by-year. For the purposes of this study, LAGs and annuli will at times be grouped together under the term "skeletal growth marker" (SGM).

Fossil Specimens

Troodon specimens described in this paper all originate from the Upper Cretaceous Two Medicine Formation and include: Museum of the Rockies (MOR) 246-11, an embryo preserved within an egg; MOR 430, a small juvenile; MOR 553, a bonebed collection representing multiple individuals of varying life stages; MOR 563, a large *Troodon* juvenile; MOR 748, a sexually mature partial skeleton, found in contact with a clutch of eggs.

Museum ID	Femur length (mm)	Femur minimal shaft circ. (mm)	Estimated body mass (kg) (calculated using methodology by Campione et al., 2014)
MOR 246-11	35	11	0.2
MOR 430-5.20-86	126	N/A	N/A
MOR 553-8.7.9.417	235	63	18.7
MOR 553-7.28.91.234	221	66	21.3
MOR 553-7.22.91.164	240	67	22.2
MOR 748-7.26.93	320	86	44.1
MOR 553-7.28.91.239	284	87	45.5
MOR 553-7.16.0.61	330	103	72.5

TABLE 1. *Troodon* femoral measurements [Planned for 2/3 page width].

Museum ID	Tibia length (mm)	Tibia minimal shaft circ. (mm)	Estimated body mass (kg) (Campione et al., 2014); (D'Emic et al., 2023)
MOR 246-11	46	N/A	N/A
MOR 430-5.20.86	160 (est.)	30	2.3
MOR 553-7.20.91.132	278	58	15.8
MOR 563-7.27.88.1	N/A	58	15.8
MOR 553-7.17.0.74	317	68	25.2
MOR 553	317	68	25.2
MOR 748-7.26.93	350	80	40.6
MOR 553-7.11.91.41	374	83	45.2
MOR 553-8.16.92-254	365	87	51.9
MOR 553-7.24.8.64	430	95	67.3
MOR 553-7.28.91.237	N/A	98 (est.)	73.8

TABLE 2. *Troodon* tibial measurements [Planned for 2/3 page width].

Only pre-existing thin sections were used for histological examination. Thin sections belonging to two *Troodon* femora and eight tibiae were analyzed under normal and circular polarized light conditions. The femora included in the dataset were those of MOR 246-11 and MOR 748 (7.26.93). The tibiae histologically examined [Fig. 2.2] included specimens from MOR 430 (5.20.86); MOR 563 (7.27.88.1); MOR 748 (7.26.93); and MOR 553, from which five tibiae were histologically examined, which include 553S-7.11.91.41, 553L-7.24.8.64, 553S-7.28.91.237, 553S-7.17.0.74, and 553S-7.20.91.132. However, a total of five femora and seven tibiae from this locality had at least basic measurements taken for the purposes of this study. As an embryo and a small juvenile respectively, thin sections from MOR 246 and MOR 430 were

mainly used as points of comparison and will not be discussed in-depth.

FIGURE 2. 2. Troodon tibia histologic growth series. [Planned for full page width].

Microscope Specifications

Histological thin sections were examined using a Nikon Optiphot 2-pol microscope equipped with Prior Optiscan II automated control system, a Nikon DS-U3 camera control unit, a Nikon DS-Fi2 color camera head, and Adobe Elements BR. Circular polarized light (CPL) conditions were achieved using a Nikon D-DP circular light polarizer. To obtain circular polarized light, the sample was interfaced with a ¼ λ plate, and then flanked by a full-λ plate, on each side. This was done to increase visibility of annuli, as the organization of fibers in annuli produces strong birefringence (H. Woodward, personal communication, 6 June, 2022) [Fig. 2.3]. Thin section slides were generally oiled before observation under CPL.

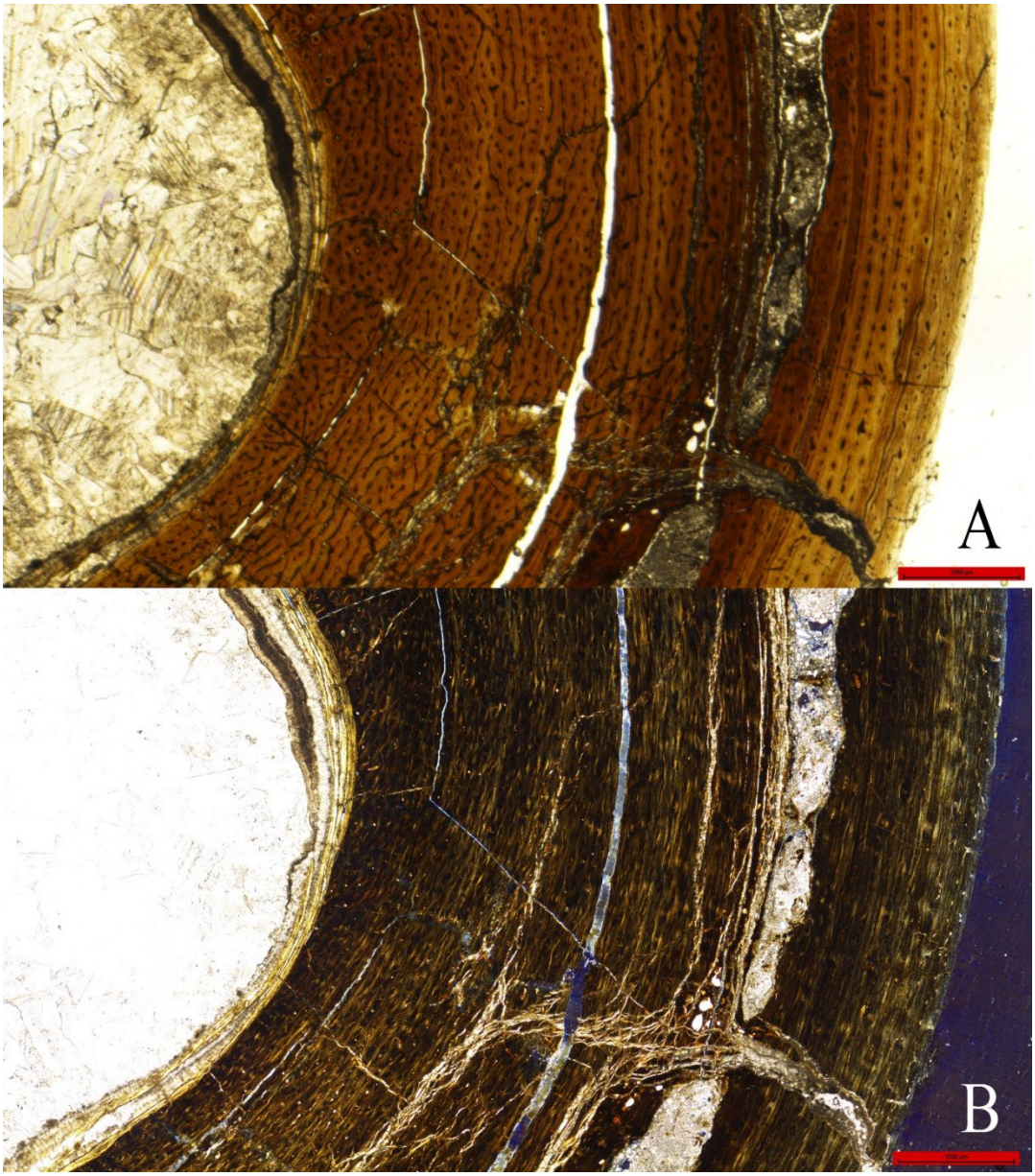

FIGURE 2. 3. MOR 748, *Troodon* tibia under **A**, normal plane; **B**, circular polarized light [planned for page width].

Histologic Aging

Bones were aged via the examination of lines of arrested growth (LAGs) and annuli visible in thin sections. Bone length and full bone circumference were measured using a standard tape measure and Exploit digital calipers. Individual growth per annum was deduced by measuring the circumferences of LAGs and annuli in Adobe Photoshop 2022.

Digital Restoration

Several thin section slides for *Troodon* were incomplete. The slides showed only partial cross-sections, largely due to bone fragmenting during the thin sectioning process. In a study such as this one, having complete or near-complete cross-sectional views of the bones is highly desirable, so methods of digital restoration were devised as a means of mitigating the damage done to the thin sections.

It should also be noted that in some instances, observable LAGs would either be partially erased by the expansion of the medullary cavity or were incomplete due to portions of the bone breaking off during preparation. In such cases, complete LAGs that were still present were used as a guide to estimate the full shape and circumference of incomplete LAGs. This was mainly used for the adult individuals (MOR 748, MOR 553S-7.11.91.41, MOR 553L-7.24.8.64, and MOR 553S-7.28.91.237).

Image Compositing— Image compositing was one of the methods used to digitally "restore" damaged thin sections. When multiple thin sections were made from the shaft of a single bone, the locations and degrees of damage present in each of the thin sections would often differ. By using Adobe Photoshop, each thin section could be made into a layer which could be placed on top of other thin sections to create a more complete cross-section of the bone. This form of digital restoration was used in the tibia and femur of MOR 748, as well as in MOR 553S-7.20.91.132 and MOR 553S-7.17.0.74. This method does contain certain flaws, as even minor changes throughout the length of a bone's shaft may lead to layers not aligning perfectly. However, when measuring the circumferences of the LAGs in each thin section, the results remained consistent.

Bone Reconstruction— For instances in which cross sections consisted of fragmented bone, Adobe Photoshop was used to select and reposition individual fragments to where they would have been located in life. Employment of this methodology was mostly constrained to MOR 553L-7.24.8.64.

Estimation of Full Cross-Sections from Cores— Some of the tibial thin sections were taken as cores, as opposed to full cross-sections. In such cases, individuals with more complete cross-sections were used to approximate the shape. Measurements of the bone's full circumference at the location of the core sample was used to determine circumference of the LAGs. By combining the shape of another individual with the full circumferential size of the core-sampled individual, approximations on the full circumferences of LAGs present in the core could be estimated [Fig. 2.4].

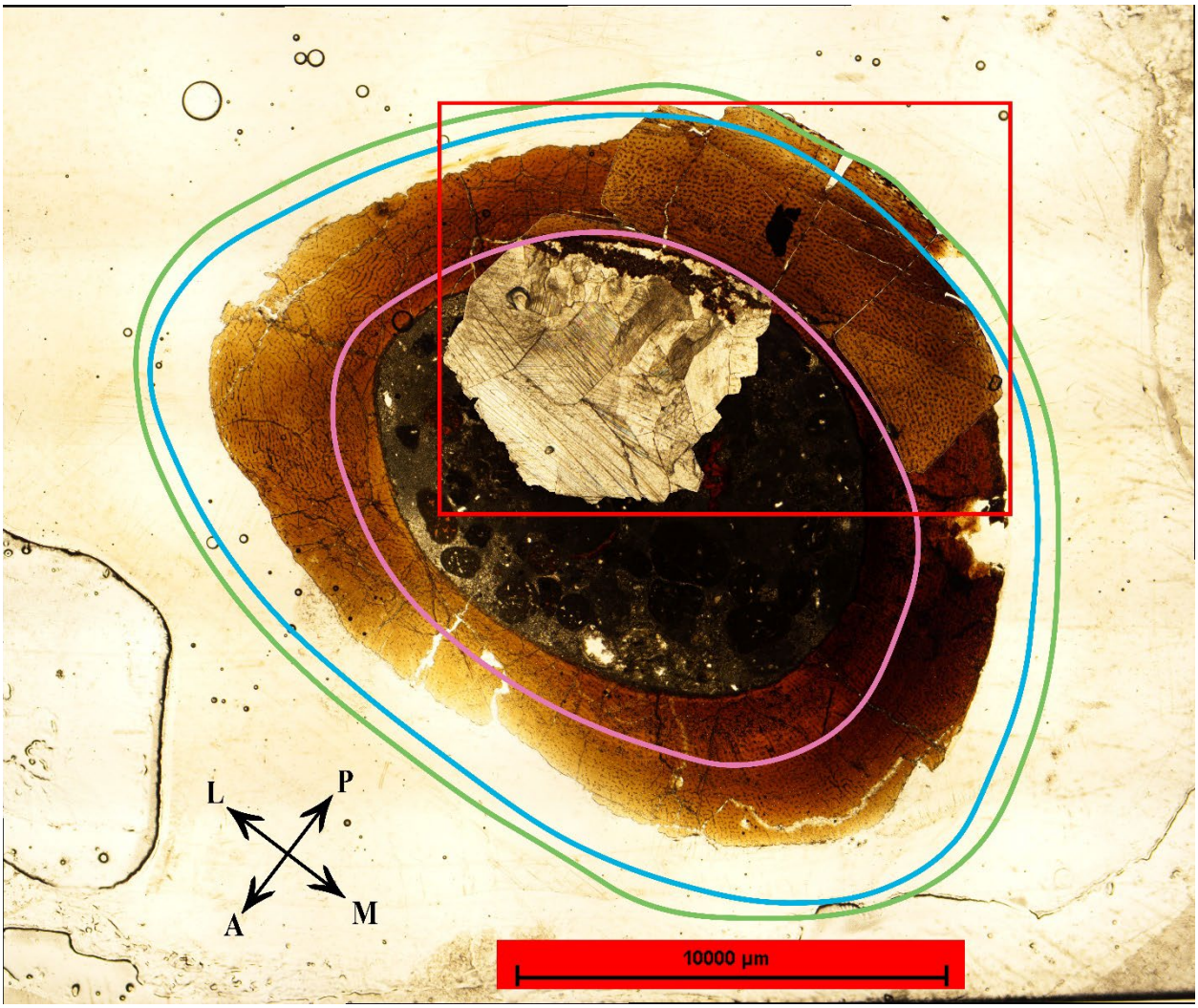

FIGURE 2. 4. *F*ragment of MOR 553S-7.17.0.74 *(red box)* superimposed onto MOR 563 to estimate full cross-sectional shape. Green line was scaled to appropriately match the full circumference of MOR 553S-7.17.0.74 at its sampling point. *The blue line indicates the estimated perimeter of the observed LAG, and the pink line indicates the medullary cavity.* [Planned for 2/3 page width].

LAGs vs. LAG-Like Structures

Not all ring-like structures observed in thin sections were counted as LAGs. Perception of the bone could be biased or skewed by pathologic, taphonomic, and methodologic alterations to the bones and their thin sections. Even at a microscopic level, it was often difficult to determine what was a true marker of annual growth and what was irrelevant. In the histological thin sections, definite LAGs were counted and measured. Annuli and various LAG-like structures

were then separately counted and measured. Various methods of implementation of the potential SGMs were then tested in an attempt to better understand which do and do not act as markers of annular growth, and to eventually create a relatively homogenous growth curve.

Despite the attempts at digital restoration, several uncertainties still remained regarding what could be considered an accurate marker of annual growth in each of the bones that had been histologically observed. Therefore, a variety of analyses were performed to potentially find patterns in ambiguous data. It was observed that definitive LAGs often produced body mass estimates very close to those produced by LAGs in other specimens. In other instances, a LAG in one specimen would correspond closely to an annulus in another specimen. Therefore, annuli were included in the final growth chart as markers of annual growth if a corresponding LAG could be found in another specimen.

Calculating Body Mass

Femoral shaft circumference has been shown to be a suitable indicator of body mass, in dinosaurs and mammals alike (Carrano, 1999), as the thickness of the femur must always be capable of supporting the weight of the organism, and histologic growth markers have been used in a multitude of studies to calculate annual growth (Chinsamy, 1994; Erickson et al, 2001; Erickson et al., 2004). An equation by Campione et al. (2014), was employed to estimate the body mass of *Troodon* individuals (W) using femoral shaft circumference (C_f).

Equation 1:

$$W = (10^{\wedge} (2.754 * \lg(C_f) - 0.683))/1000$$

Most of the bones that underwent histological examination were not femora, but tibiae. A recent study by D'Emic et al. (2023), found a way to approximate femoral circumference based on the minimum circumference of the tibial shaft (C_t).

Equation 2:

$$C_f = \exp(\exp((1.0586697*\ln(\ln(C_t))-0.07719615))$$

By combining the two equations, we were able to use tibial circumference to estimate body mass.

Equation 3:

$$W = (10\text{^}(2.754*\lg(\exp(\exp((1.0586697*\ln(\ln(C_t))-0.07719615))))-0.683))/1000$$

Due to variations in sampling location, many of the histological samples that were examined had circumferences that were greater than the minimum shaft circumference of the bone they originated, which would result in overestimations of the body mass estimates produced by the circumferences of SGMs. To correct for this variance, body mass estimates were reduced, at each age relative to the difference between the circumference of the histologic sample (C_h) and the actual minimum shaft circumference of the bone. In the previous three equations, SGMs could be used in place of C_t and C_f to calculate body mass at specific ages. However, the following equation requires a distinction between full bone circumferences and those of SGM. Therefore, C_t has been used to designate where full circumference is necessary, and C_s has been used to indicate where the circumferences of SGMs may be used.

Equation 4:

$$W= (10\text{^} (2.754*\lg(\exp(\exp((1.0586697*\ln(\ln(C_s*(C_t/C_h)))-0.07719615))))-0.683))/1000$$

The same corrections can be inserted to Equation 1 when using the histologic samples and SGMs of femora to calculate body mass by replacing C_f with (C_s*(C_f/C_h). (See Appendix A for full list of observed SGMs and body mass estimates).

Among the *Troodon* fossils observed was MOR 246-11, an egg containing several bones from a nearly fully-developed embryo. A study by Varricchio et al. (2013) was able to approximate what the mass of the "ideal" *Troodon* egg would have been (prior to fossilization). Incorporating that estimate into Deeming and Birchard's (2006) equation relating avian initial egg mass (IEM) to the mass of the hatchling it would produce (HM), the body mass for a *Troodon* hatchling was able to be estimated.

Equation 5:

$$HM = 0.701 * IEM^{0.987}$$

Cross-Sectional Shape—The tibiae that were observed histologically, were originally thin sectioned with the intent of keeping the location homogenous between individuals. However, the minor differences that remained between locations resulted in the thin sections generally having one of two distinct shapes [Fig. 2.5]. Difference in shape of the tibial cross-section ultimately did not significantly impact measurements, and thus did not need to be factored into results.

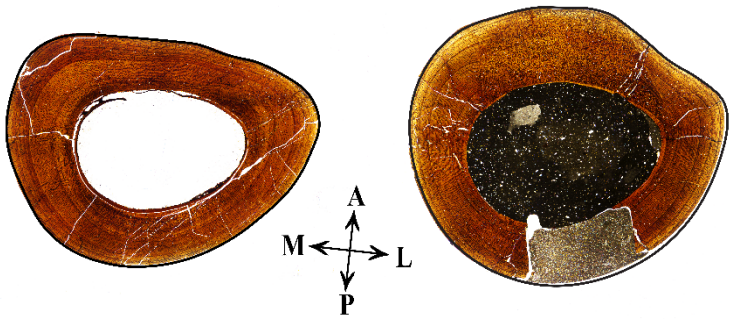

FIGURE 2. 5. Examples of the two tibial cross-sectional shapes observed, from MOR 553S-7.11.91.41 (left) and MOR 553S-7.28.91.237 (right), in addition to extensive secondary remodeling. Remodeling was observed to occur in samples taken more distally along the tibial shaft. **Abbreviations: a**, anterior; **p**, posterior; **m**, medial; **l**, lateral [Planned for page width].

Scaling for Ontogeny—Traditionally, estimating the body masses of individuals of various ontogenetic stages would make use of an equation by Erickson and Tumanova (2000), in which the body mass of the largest individual is found, and then smaller individuals are scaled proportionally based on the cube of their femur length. However, application of this methodology performed on a handful of juvenile emus resulted in less accurate estimates of body mass [Table 3]. Searches through the existing literature found no actualistic testing verifying the validity of Erickson and Tumanova's technique. Therefore, it was decided that Erickson and Tumanova's ontogenetic scaling exponent would not be incorporated when calculating juvenile body mass.

Specimen ID	Age (days)	Esimated Body Mass (Anderson et al., 1985) (kg)	for Ontogeny (Erickson & Tumanova, 2000) (kg)	Actual Body Mass (kg)	Mass at Time of Hatching (kg)
HRB-006	19	1	0.52	N/A	0.43
HRB-034	N/A	19.7	22.6	19.6	N/A
HRB-037	N/A	14.7	17.8	14.5	N/A

TABLE 3. Comparison of juvenile emu body mass estimation methods. While the actual body mass of HRB-006 is not known, given the daily body mass increases of emu chicks documented by Suganya et al. (2017), the estimation calculated using the methodology of Anderson et al. (1985) would be approximately two standard deviations below the mean of 19-day-old individuals. Incorporation of Erickson and Tumanova (2000) produces an estimate more than 11 deviations below the mean.

RESULTS

Bone-By-Bone Analysis (Smallest to Largest)

MOR 563—MOR 563 [Fig. 2.6] is a partial tibial shaft originating from a young juvenile. The bone is in poor condition compared to most of the other tibiae examined in this study. MOR 563 is mainly comprised of laminar bone and does not have any clear LAGs under normal light conditions, but under CPL one faint annulus is visible. Lacking any other visible SGMs, we interpret this to represent a year-one SGM.

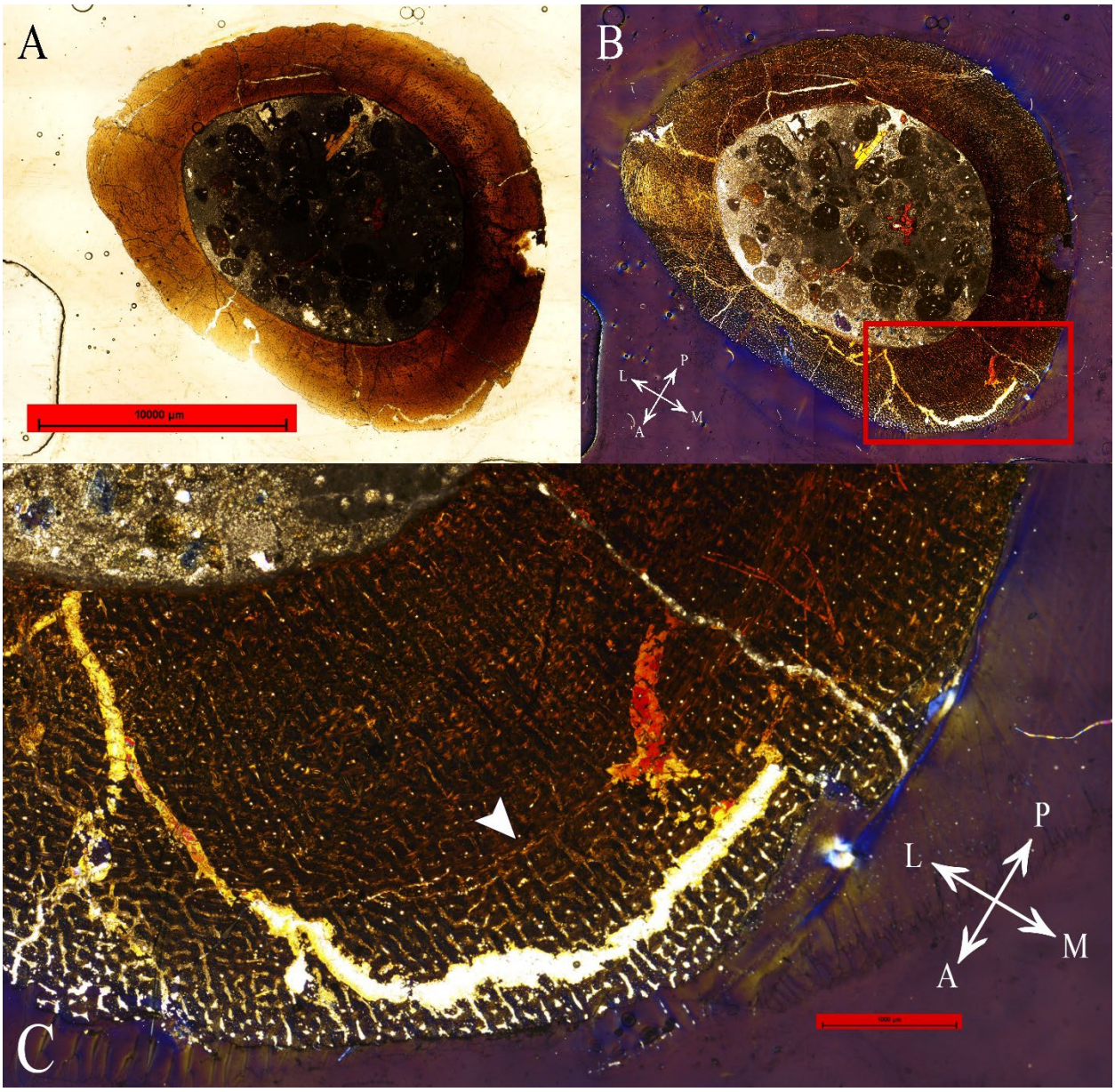

FIGURE 2. 6. The tibia of MOR 563 **A**, under normal plane light; **B**, under circular polarized light; **C**, close-up with arrow indicating an annulus. **Abbreviations: a**, anterior; **p**, posterior; **m**, medial; **l**, lateral [Planned for full page width].

MOR 553S-7.20.91.132 — MOR 553S-7.20.91.132 [Fig. 2.7] is a core sample in which two clear LAGs are present. The periosteal surface of the bone is located approximately 0.3mm - 0.6mm outside of the second LAG. While not visible in the thin section slide pictured, a second LAG was observable on the anterior half of other thin section samples of this bone. This bone

mostly consists of longitudinal bone and possesses a spongy periosteal edge indicative of rapid growth at time of death.

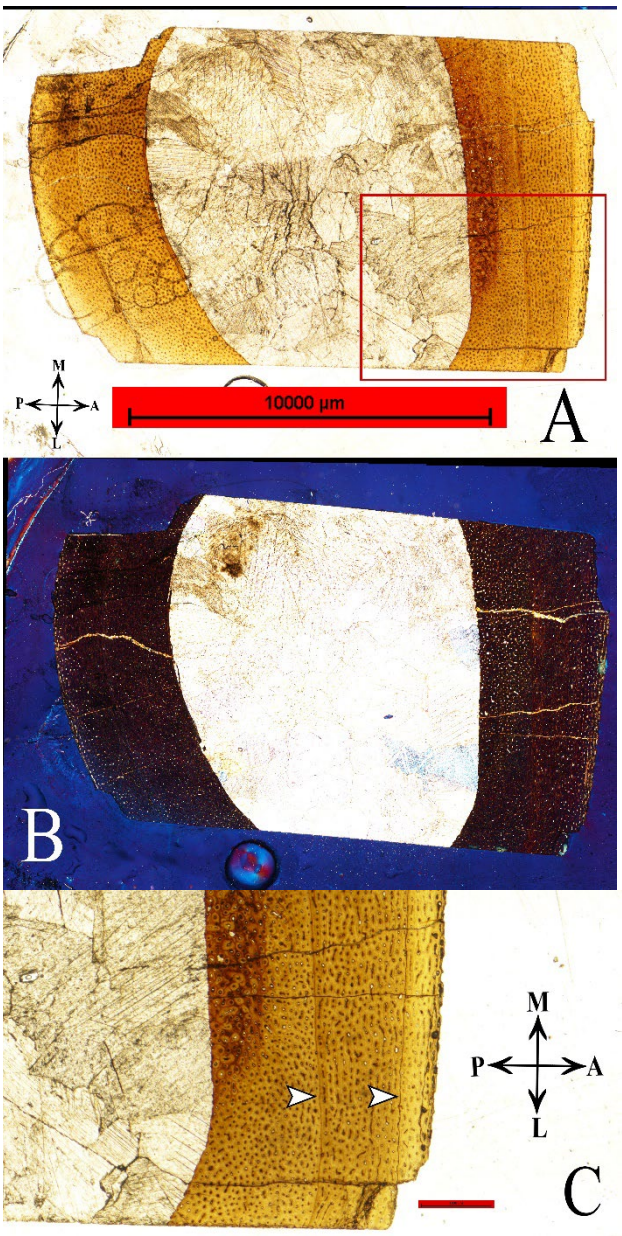

FIGURE 2. 7. MOR 553S-7.20.91.132 **A**, under normal plane light; **B**, under circular polarized light; **C**, close-up with arrows indicating LAGs. Though not visible in this thin section, the second LAG is visible on the posterior half of the core in other slides. **Abbreviations: a**, anterior; **p**, posterior; **m**, medial; **l**, lateral [Planned for column width].

MOR 553S-7.17.0.74 —Only half of a typical core sample remains in this bone's thin section slides [Fig. 2.8], resulting in only approximately a quarter of the bone's cross-section being available for histologic observation. The sample is made up largely of longitudinal bone. Depending on the specific thin section slide, one to two LAGs are present toward the periosteum. The two potential LAGs are unusually closely-spaced during what was observed to be a period of rapid growth in other individuals. In addition, with how fragmentary the periosteal surface is, the outermost of these two LAGs may be no more than an unusually-shaped crack. Therefore, it was decided that only the innermost of these LAGs would be counted, as it was the more certain of the two. Like MOR 553S-7.20.91.132, the spongy texture of the periosteal surface of this bone indicates that the individual was still rapidly growing. All of the thin sections belonging to MOR 553S-7.17.0.74 possess a displaced wedge-shaped chunk of bone that is present toward the endosteal surface. The shape of the wedge makes it difficult to discern both where it originated from, as well as its potential relevance to determining the circumference of LAGs. Using the digital restoration methods detailed earlier, we were able to approximate the appearance of a full cross-section. The LAG produced a body mass estimate consistent with that of the third LAG in the tibia of MOR 748, the second LAG of MOR 748's femur, the second LAG of MOR 553S-7.11.91.41, and the innermost LAG of MOR 553S-7.28.91.237. We interpret this LAG as being the individual's third, with the first two being lost either from expansion of the medullary cavity, lost during the thin sectioning process, or represented by one of the boundaries of wedge-shaped chunk that could not be placed.

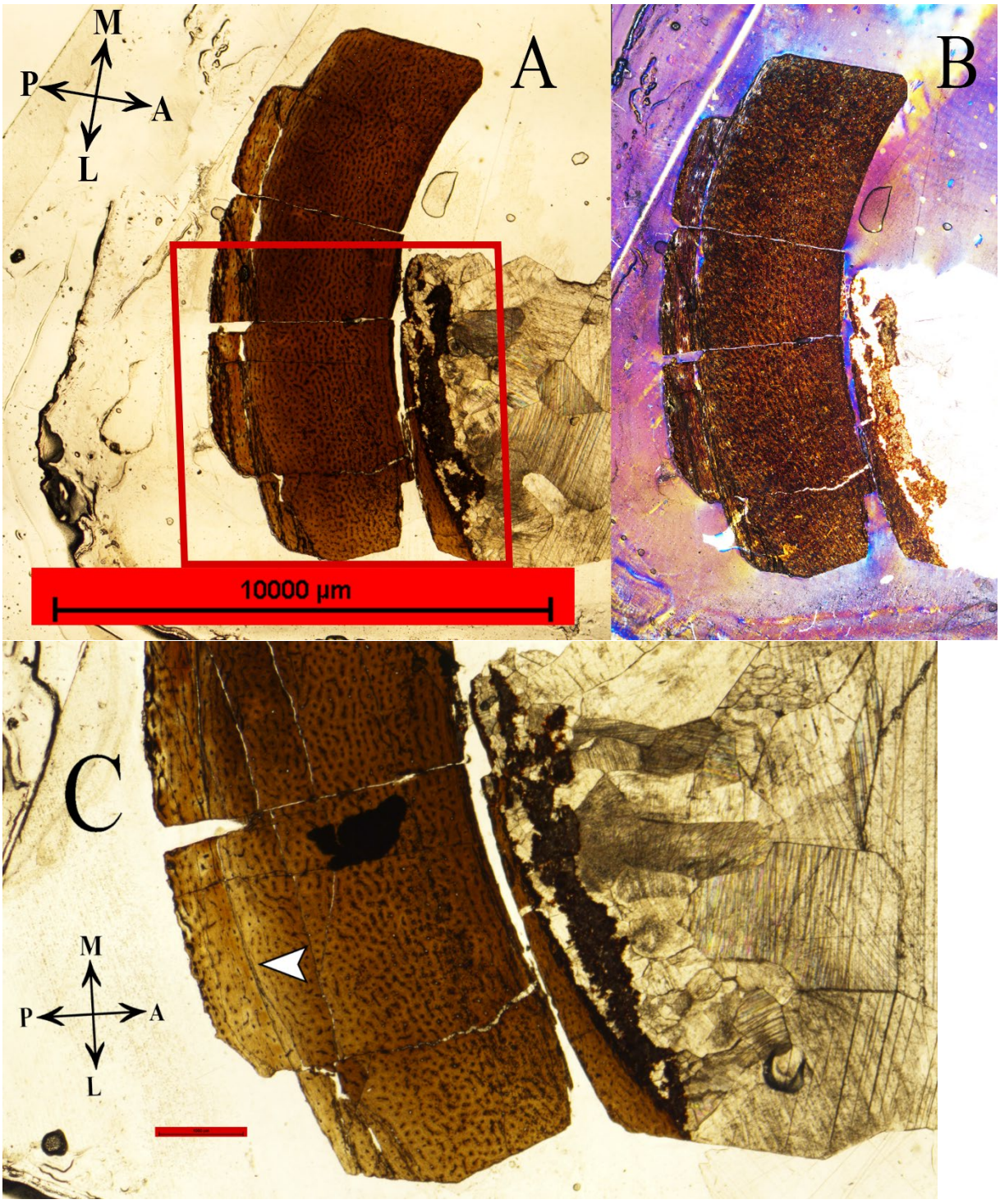

FIGURE 2. 8. MOR 553S-7.17.0.74 **A**, under normal plane light; **B**, under circular polarized light; **C**, close-up with arrow indicating LAG. **Abbreviations: a**, anterior; **p**, posterior; **m**, medial; **l**, lateral [Planned for column width].

MOR 748—The tibia of MOR 748 [Fig. 2.9] was subject to heavy taphonomic damage by apparent root and fungal intrusion (Varricchio et al., 2008). It also possessed a large quantity of circumferential cracks, making it particularly difficult to age, even with the assistance of CPL. Unlike the other individuals observed, both the tibia and the femur of MOR 748 were sampled histologically. Despite the taphonomic damage, the LAGs of the two bones were able to be cross-referenced with one another to come to a consensus on where the individual's LAGs were located. Less-certain SGMs were only included in the final growth curve if they could be correlated to more definitive LAGs of other individuals. In the end, four potential SGMs observed were not included in the final results due to either a lack of correlation to SMGs observed in other individuals, or due to the presence of a separate potential SGM that corresponds to those of other individuals more closely. Toward the anterior surface of 748's tibia are two layers reflecting rapid bone modeling. Upon further inspection, it was found that both layers seem to emerge from a single multi-LAG. It is possible that these features represent biometrically adaptive bone modeling (Cubo et al., 2015). Such growths are generally used to increase a bone's structural support in response to injury in another bone, most likely the fibula in this instance. Unfortunately, MOR 748 only possesses a partial fibula, and no signs of injury or pathology are visible in what fragments are available. Another possibility is that these layers of bone represent an acute muscle attachment point. The observed emergence of the layers from a single multi-LAG would be expected for muscle attachment. Comparison to other tibiae shows some evidence of periosteal growth in similar areas, but not nearly as extensively as in MOR 748.

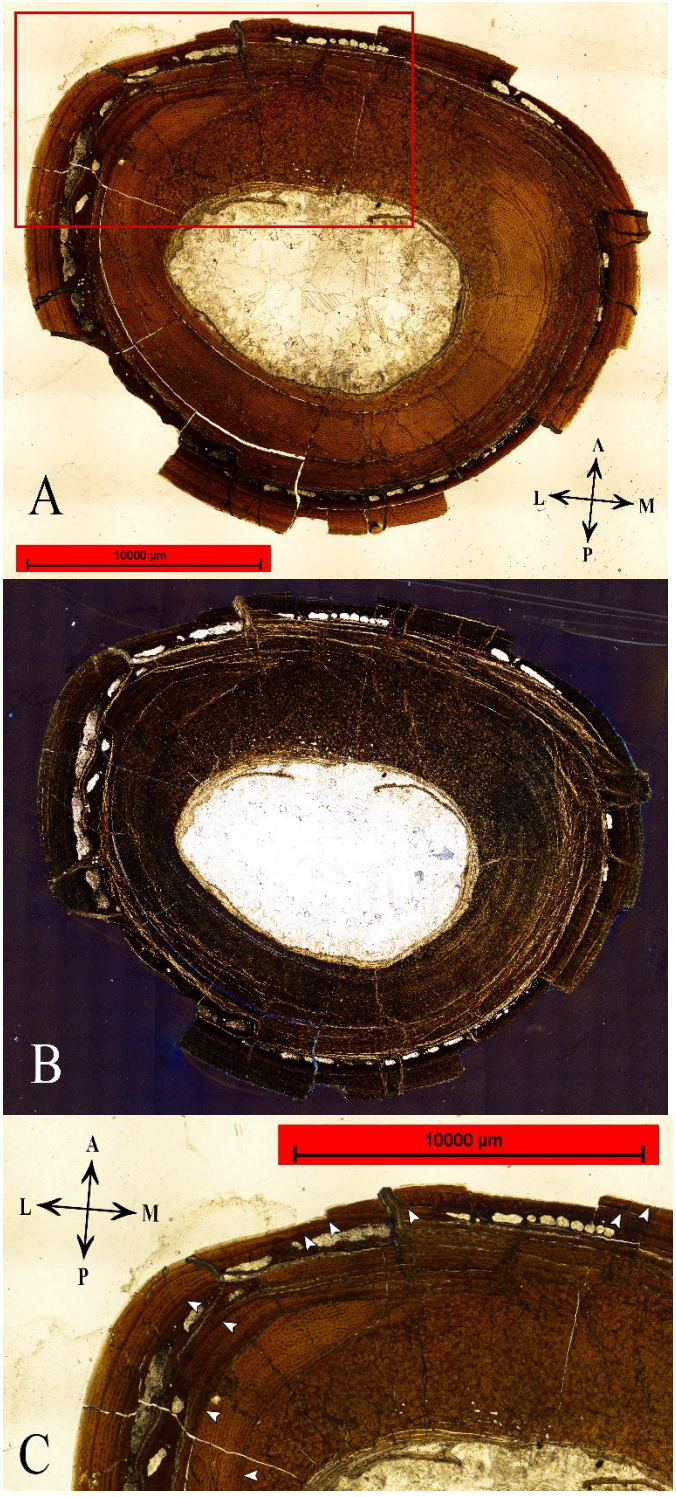

FIGURE 2. 9. The tibia of MOR 748 **A**, under normal plane light; **B**, under circular polarized light; **C**, close-up with arrows indicating locations of LAGs. **Abbreviations: a**, anterior; **p**, posterior; **m**, medial; **l**, lateral [Planned for 2/3 page width].

Like the tibia, the femur of MOR 748 [Fig. 2.10] has undergone heavy taphonomic damage and possesses higher degrees of parallel-fibered and lamellar bone compared to many of the other specimens. It is believed that the innermost LAG of the femur was lost from expansion of the medullary cavity, as the first observable LAG corresponds most closely to the second LAG of the tibia. Four potential SMGs were excluded from the final analysis of growth, though only two of these correspond to potential SGMs that were found in and excluded from the growth analysis of the tibia. One annulus visible in the specimen produced a body mass estimate closely matching a LAG visible in the tibia and was thus counted as a true marker of annual growth. Body mass calculations performed based on the femur and tibia of MOR 748 gave slightly differing results. Estimation of femoral circumference using tibial circumference resulted in an underestimation of about 3.6 mm, which in turn led to a difference in estimated body mass of approximately 3.6 kg. We attribute these differing estimates to be due to the poor condition of the periosteal surfaces of 748's femur and tibia, as several layers of growth are almost entirely absent from histologic thin sections in both bones.

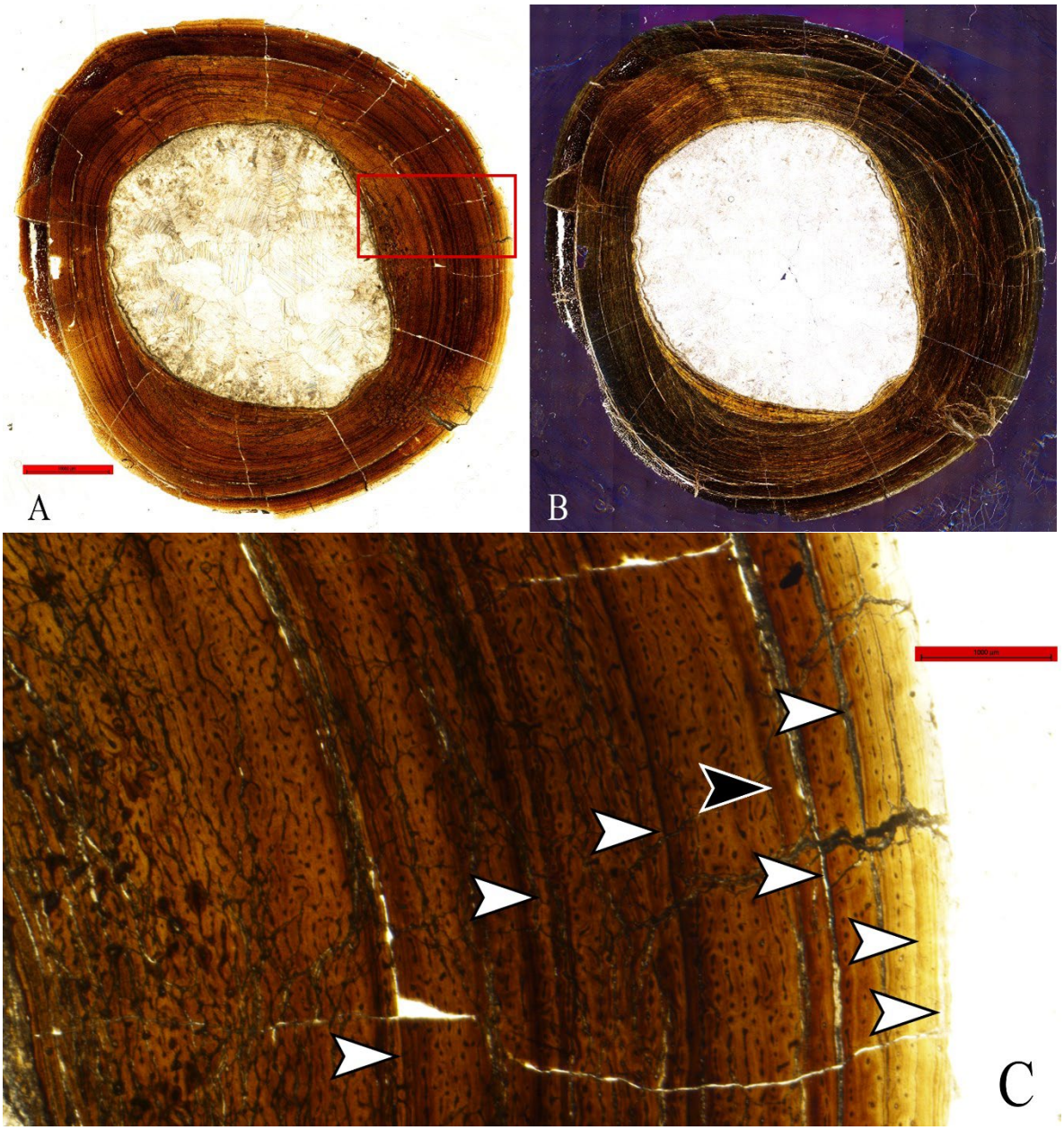

FIGURE 2. 10. The femur of MOR 748 **A**, under normal plane light; **B**, under circular polarized light; **C**, close-up with arrows indicating SGMs counted as markers of annual growth. White arrows indicate LAGs, black arrows indicate annuli [Planned for 2/3 page width].

MOR 553S-7.11.91.41 — MOR 553S-7.11.91.41 [Fig. 2.11] appears to belong to an adult-aged individual, with the beginnings of an EFS present toward the periosteal surface. Of the tibiae included in the dataset, it is the most well-preserved, having both a complete bone as

well as full, largely undamaged thin sections. It possesses a distinct lack of extensive secondary remodeling on its anterior side, possibly due to differences in the sampling location of the thin sections. As samples displaying the remodeling tend to be located more distally, the remodeling may be the result of the attachment of the ascending process of the astragalus. While some minor remodeling is present in this specimen, this is likely to be the result of muscle scarring. Examination of this tibia under CPL reveals three potential annuli without associated LAGs. The circumferences of the annuli are all indicative of body masses, similar to those demarcated by true LAGs present in other specimens. Inspection of the EFS, shows what at first appears to be as many as eight LAGs present on the posterior periosteal surface converge into two to three LAGs anteriorly. Similar multi-LAGs were observed toward the periosteum of other adult specimens as well. Multi-LAGs, such as these were only counted as singular LAGs. Even with the reduced number of LAGs, the periosteal region of the bone displayed a transition from laminar fibrolamellar to lamellar bone. Therefore, it was concluded that the specimen had reached somatic maturity.

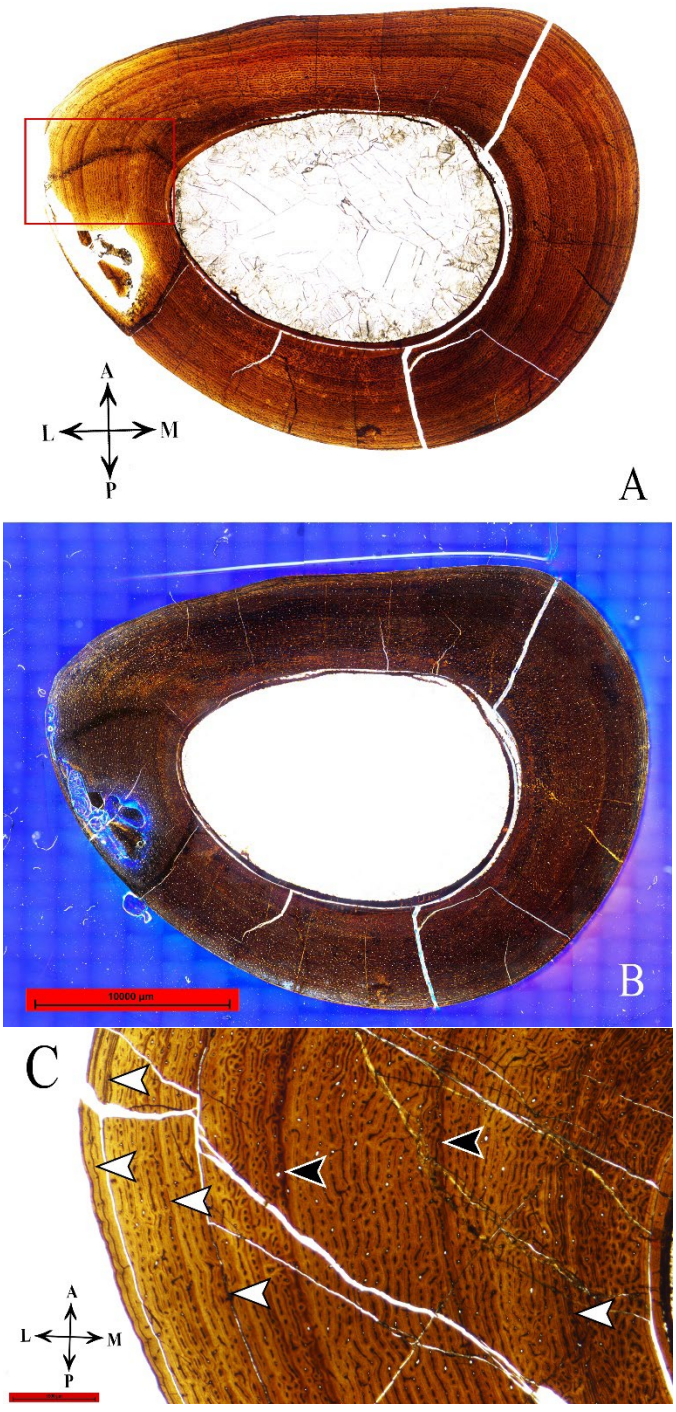

FIGURE 2. 11. MOR 553S-7.11.91.41 **A**, under normal plane light; **B**, under circular polarized light; **C**, close-up with arrows indicating SGMs counted as markers of annual growth. White arrows indicate LAGs, black arrows indicate annuli. **Abbreviations: a**, anterior; **p**, posterior; **m**, medial; **l**, lateral [Planned for column width].

MOR 553L-7.24.8.64 — MOR 553L-7.24.8.64 [Fig. 2.12] is extensively crushed. Despite its condition, large portions of the medial and lateral sides of the bone remain intact.

FIGURE 2. 12. MOR 553L-7.24.8.64 close-up with arrows indicating LAGs. **Abbreviations: a**, anterior; **p**, posterior; **m**, medial; **l**, lateral [Planned for 2/3 page width].

A digital reconstruction of the bone was attempted in Adobe Photoshop, but portions of the cross-section were still missing, likely proximodistally displaced after the bone was crushed [Fig. 2.13]. In what portions of the periosteal surface remain, there appears to be an EFS present following the sixth visible LAG.

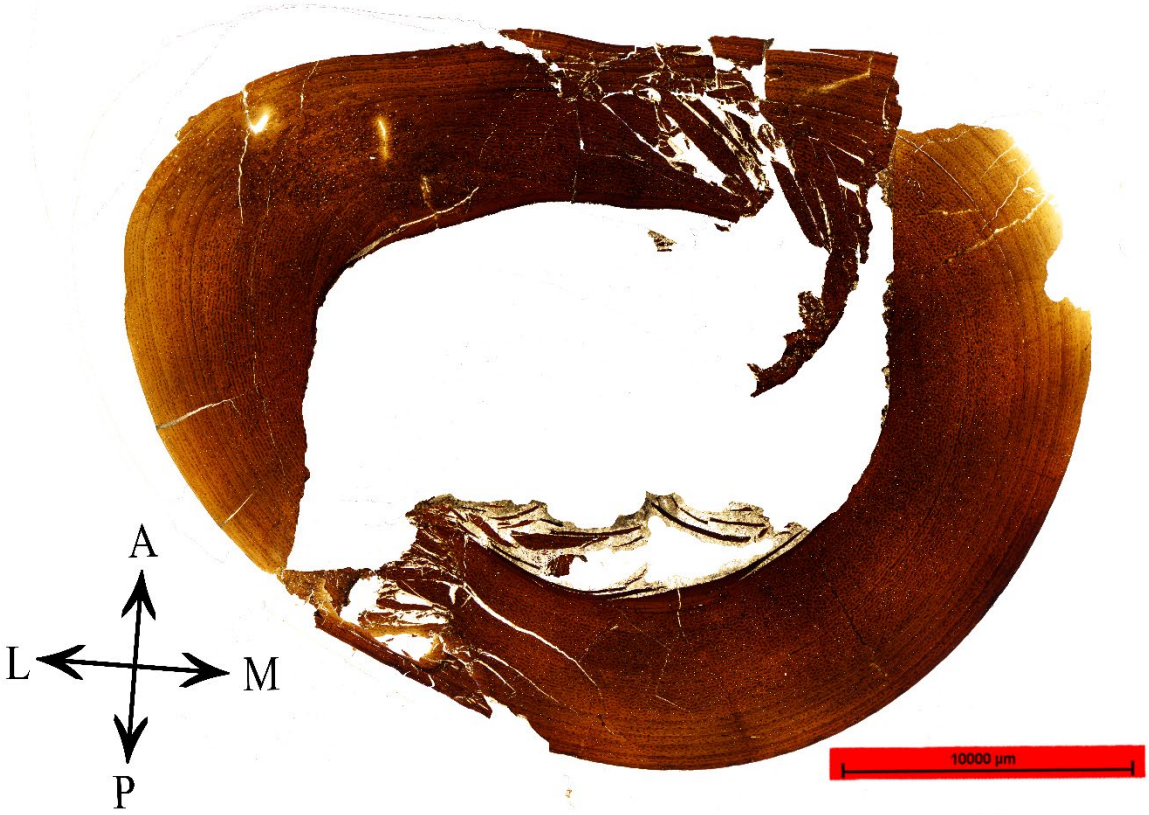

FIGURE 2. 13. Attempted digital reconstruction of MOR 553L-7.24.8.64. Pieces were positioned within an area possessing a circumference matching that of the bone at its sampling location. [Planned for column width].

MOR 553S-7.28.91.237— MOR 553S-7.28.91.237 [Fig. 2.14] is a fragment representing the distal shaft of a tibia. Thin sections were taken from the proximal end of the fragment, a location which corresponds to the area of the tibia which generally possesses the minimal shaft circumference. As a result, the location sampled can be considered suitable for the purposes of this study. MOR 553S-7.28.91.237 is possibly the most robust tibia in the dataset, only comparable to MOR 553L-7.24.8.64. However, estimates for the minimal shaft circumference for MOR 553L-7.24.8.64 come out to approximately 95mm, whereas that of this bone is 98mm. The medullary cavity of MOR 553S-7.28.91.237 has a perimeter larger than the full circumference observed in other individuals at their second LAG, and an innermost LAG with a

circumference close to that of the third LAG in smaller specimens. It is likely that histologic evidence of the LAGs from the first two years of this individual's life was erased by expansion of the medullary cavity. MOR 553S-7.28.91.237 experienced incredibly rapid growth during the time period between its second and third visible LAGs (representative of the fourth and fifth year of life). The growth observed at this time is highly reminiscent of the growth observed prior to the innermost LAG of MOR 553L-7.24.8.64. However, under CPL conditions, there are large areas of bone that possess minor to moderate degrees of relatively more parallel-fibered bone, indicative of long periods of time during which growth had slowed down, if only slightly.

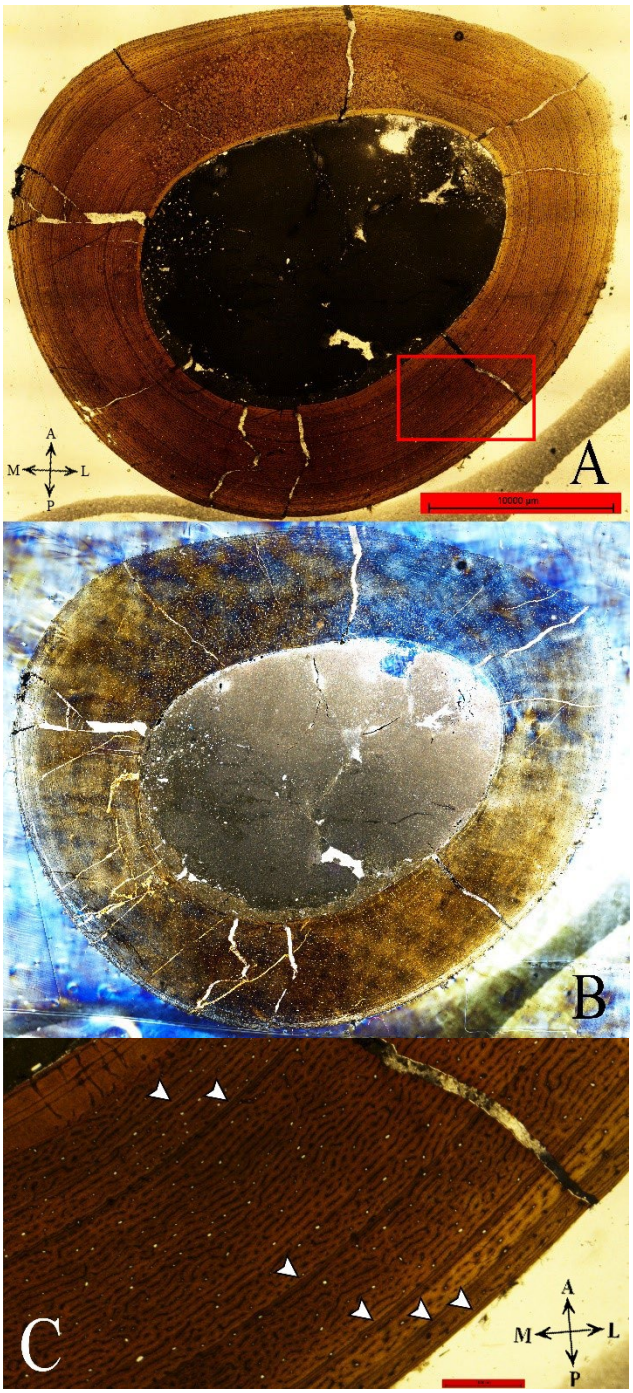

FIGURE 2. 14. MOR 553S-7.28.91.237 **A**, under normal plane light; **B**, under circular polarized light; **C**, close-up with arrows indicating LAGs. **Abbreviations: a**, anterior; **p**, posterior; **m**, medial; **l**, lateral [Planned for 2/3 page width].

Further Observations— MOR 553L-7.24.8.64 and MOR 553S-7.28.91.237 are far more robust than MOR 553S-7.11.91.41 and the tibia of MOR 748. However, the rates at which MOR 553L-7.24.8.64 and MOR 553S-7.28.91.237 grew year-by-year initially appeared to have differed significantly. Following its year of most rapid growth, MOR 553L-7.24.8.64 grew at a somewhat slow, but constant rate, increasing by approximately 3-5 kg every year for five years. Following the most rapid year of growth in MOR 553S-7.28.91.237, its growth rate decelerated annually until it developed a typical EFS.

One pattern observed in many specimens was an abundance of multi-LAGs toward the periosteal surface of bones. As a result, it was often difficult to interpret how many years were being represented by any given EFS. While double-LAGs would occasionally occur within the early years of rapid growth, toward the outermost edge of the larger specimens would be one or more LAGs that would diverge and split into as many as four or five LAGs. These LAGs were not observed toward the periosteum of juvenile or subadult specimens. The two forms of these multi-LAGs (singular and split) were observed to occur in similar locations between specimens. Anteriorly, they would be “singular” and posteriorly would be “split”. In MOR 748, these multi-LAGs continued to diverge and expand into crescent-shaped bulges of remodeled bone [Fig. 2.15].

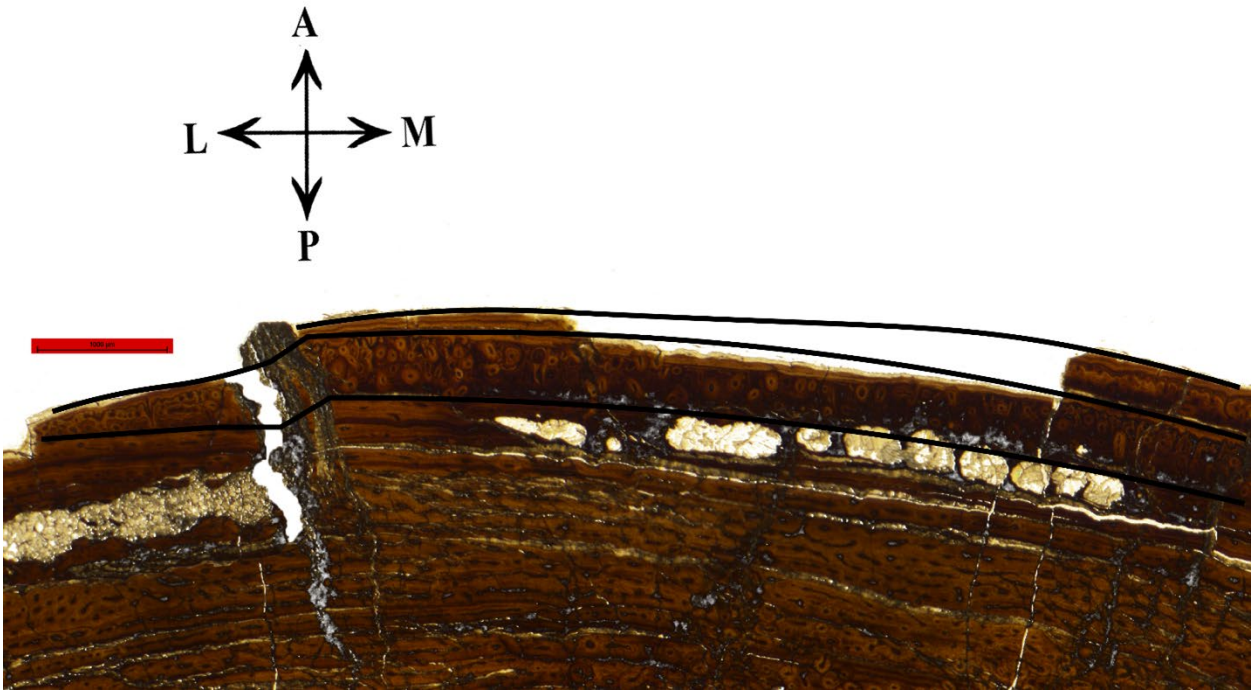

FIGURE 2. 15. Unusual bone growth observed toward the posterior periosteum of the tibia of MOR 748, marked by black lines. **Abbreviations: a**, anterior; **p**, posterior; **m**, medial; **l**, lateral [Planned for column width].

Body Mass of Troodon formosus

The body mass of a hypothetical *Troodon* hatchling was estimated to be approximately 223.6 g. Based on the femur, the adult individual MOR 748 was calculated to be around 44 kg. A more unexpected result of this study was the maximum adult body mass of *Troodon.* While Varricchio had estimated an adult body mass of 50 kg for *T. formosus,* as many as three individuals in this study greatly outweighed that estimate, with the largest having an estimated body mass of approximately 73.8 kg. However, this difference is merely a reflection of the differing methodologies used to calculate body mass [Table 4]. Both MOR 748 and the similarly-sized MOR 553S-7.11.91.41 possess external fundamental systems, and are thus believed to have reached somatic maturity. As stated previously, the tibia and femur of MOR 748 possess several features that may or may not be SMGs. If we were to account all of these

features as true markers of annual growth [Fig. 2.16], MOR 748 would have reached an adult body mass similar to that of MOR 553S-7.11.91.41, though would have taken several more years to reach that size. However, all of the LAGs and annuli observed in MOR 553S-7.11.91.41 correspond closely enough to SGMs observed in MOR 748 to indicate a pattern of growth slowing at particular body sizes across individuals [Fig. 2.17].

Museum ID	Body Mass (Anderson et al., 1985) (kg)	Body Mass (Campione et al., 2014) (kg)
MOR 748-7.26.93	30.57	44.12
MOR 553S-7.28.91.239	31.55	45.54
MOR 553S-8.7.9.417	13.07	18.72
MOR 553S-7.16.0.61	50.02	72.50
MOR 553S-7.28.91.234	14.84	21.28
MOR 553S-7.22.91.164	15.46	22.18
MOR 553S-7.11.91.41	31.55	45.20
MOR 553S-8.16.92.254	35.67	51.92
MOR 553S-7.17.0.74	17.43	25.15
MOR 553S-7.28.91.237	50.02	73.76
MOR 553S-7.20.91.132	11.03	15.77
MOR 553L-7.24.8.64	46.14	67.30
MOR 430-5.20.86	3.17	2.31
MOR 563	9.48	13.54

TABLE 4. Comparison of *Troodon* body mass estimates by methodology [planned for column width].

The smallest SGMs observed indicated body masses averaging at 8.0 kg. We interpret this to potentially represent the range of body masses in year-old individuals. However, this

cannot be stated definitively as the tibial cross-section of the only individual younger than one year old, MOR 430, is small enough to fit into the medullary cavity of the next smallest specimen. Therefore, it is entirely possible that expansion of the medullary cavity erased SGMs even in juvenile specimens. The second LAGs of two individuals produced body mass estimates averaging 12.4 kg, so we interpreted those to be year-two LAGs. Two other bones possessed innermost LAGs that produced body mass estimates close to those of these LAGs (likely due to the expansion of the medullary cavity erasing their first LAG), and so we implemented those into the body mass estimates of two-year-old individuals to get a new range of 11.4 to 14.4 kg and an average of 12.6 kg. Using similar correlative methods, the body mass average for year three was determined to be 20.6 kg, and year four to be 26.6 kg. After this point, the growth trajectories of some individuals began to diverge. MOR 553S-7.11.91.41 and MOR 748, grew relatively slowly, both eventually topping off at about 45kg by the eighth or ninth year of life. The two innermost LAGs of MOR 553S-7.28.91.237 produced body mass estimates of 21.7 kg and 26.8 kg, and thus we interpreted them to represent the third and fourth-year LAGs respectively. Following this, the individual nearly doubled its mass in the span of one year, with its year-five LAG producing a body mass estimate of 46.4 kg. It then continued to grow at rates far faster than those of MOR 748 and MOR 553S-7.11.91.41. At approximately eight years of age, MOR 553S-7.28.91.237 had reached a circumference indicative of an individual weighing 73.8kg.

FIGURE 2.16. Graph of *Troodon* growth rates with the inclusion of all potential SGMs observed in MOR 748 [planned for full page width].

MOR 553L-7.24.8.64 grew to have a very similar final body mass to MOR 553S-7.28.91.237 at 67.3 kg, though its annual growth rates were highly unusual compared to the other three adult individuals. Even estimating the year represented by the innermost LAG could not be performed confidently. Its medullary cavity was only large enough to erase evidence of two LAGs, yet its innermost LAG produced a body mass estimate of 41.9 kg, a weight reached upon the fifth year in the most comparable individual, MOR 553S-7.28.91.237.

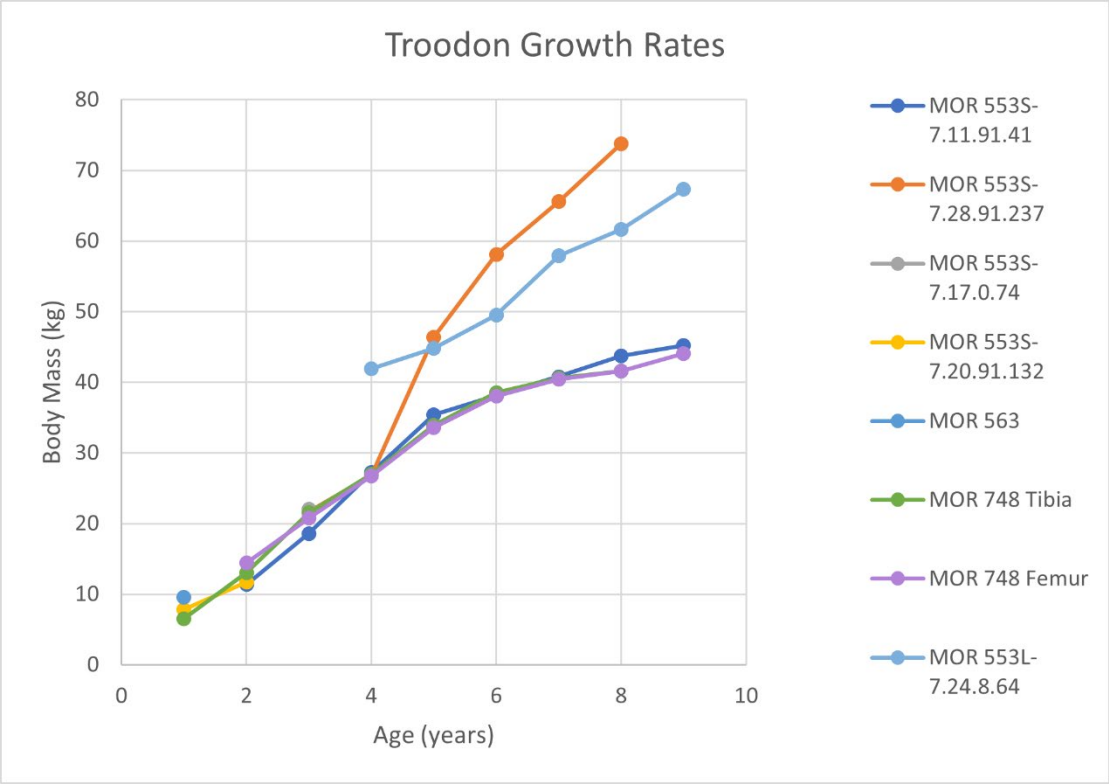

FIGURE 2. 17. Final histological growth chart of *Troodon formosus*, excluding potential SGMs that did not correspond to those of any other individual. [Planned for full page width].

DISCUSSION

Growth in *Troodon*

Of the adult individuals that were histologically examined, two of them appeared to follow very similar growth trajectories, and two individuals grew to much larger sizes but took very different paths to get there. MOR 553L-7.24.8.64 displayed highly unusual growth patterns relative to the other Troodon observed. The innermost observable LAG has the circumference of an individual with a body mass of 42 kg, which is roughly equal to the full body masses of the two smaller adult individuals. The other three adult-aged Troodon individuals (MOR 553S-7.11.91.41, MOR 748, and MOR 553S-7.28.91.237) displayed growth patterns typical of species with determinate growth in that they experience relatively rapid growth until sexual maturity,

after which point growth rates decelerate annually until it has ceased entirely. In MOR 553L-7.24.8.64, following the innermost LAG, the spacing between all subsequent LAGs indicate increases in body mass anywhere between 2.9 and 8.4 kg per year up until the formation of the EFS, with no discernable pattern present.

Throughout the *Troodon* fossils observed, growth seemed quite consistent among juveniles, though adults showed high degrees of variation. Forelimb bones attributed to *T. formosus* have shown similar degrees of variation. Some humeri display juvenile features while other, similarly-sized humeri display adult features (DJV, personal observation). High degrees of intraspecific size variation have also been reported in the Triassic theropod *Coelophysis bauri*, though Barta et al. (2022) attributes it to harsh environmental conditions.

Whether the variability in sizes observed here is the result of sexual dimorphism or represents normal individual variation is uncertain, though we are inclined to lean toward the former. Up to three individuals possessed body masses ranging between 67.3 and 73.8 kg, and up to three had body masses between 40.6 and 45.5 kg. Only a single bone in the dataset fell between these ranges at 51.9 kg, though this may also be considered close enough to the smaller adults to be a part of that group. Unfortunately, due to time constraints, it could not be histologically examined [Fig. 2.18].

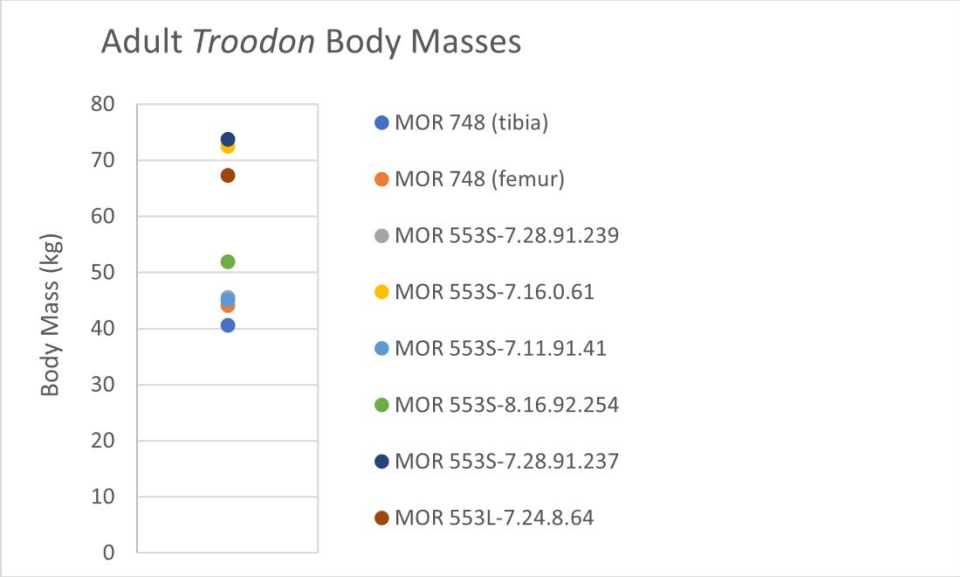

FIGURE 2.18. Distribution of adult body masses in *Troodon* [planned for column width].

CONCLUSION

New methodologies for estimating the body mass of extinct organisms have yielded surprising results with the revelation that several *Troodon formosus* individuals may have possessed body masses greatly surpassing previous estimates. Histologic examination of a multitude of femora and tibiae found the development of external fundamental systems in multiple individuals estimated to only be 40-45 kg, despite other individuals reaching over 70 kg before developing an EFS. Despite mostly homogenous growth during the early years of life, growth rates diverge at around four years of age. We interpret this split to represent the onset of sexual maturity, eventually resulting in sexually dimorphic sizes.

ACKNOWLEDGEMENTS

I would like to thank Allison Gentry and Ellen Lamm for producing the thin sections used in this study; Dr. Michael D'Emic for advance notice on the tibia-femur circumference equation; Dr. Holly Woodward for histology imaging advice; my graduate cohort for being such

an effective escape from work; to Dr. John Scannella and Museum of the Rockies for the loan of Troodon specimens; the Blackfeet Nation, the families of Lewis Carroll, Vernon Carroll, Huey Monroe, MOR inc., The Nature Conservancy, and the Peebles families for permission to excavate and collect the fossils from their land; the National Science Foundation for funding John Horner's field work when these specimens were collected; and Montana State University's Department of Earth Sciences. Finally, I would like to thank my parents for their tireless support and understanding.

LITERATURE CITED

Barta, D. E., Griffin, C. T., & Norell, M. A. (2022). Osteohistology of a Triassic dinosaur population reveals highly variable growth trajectories typified early dinosaur ontogeny. Scientific reports, 12(1), 17321-17321. https://doi.org/10.1038/s41598-022-22216-x

de Buffrénil, V., & Quilhac, A. (2021). Bone Tissue Types: A Brief Account of Currently Used Categories. In V. de Buffrénil, A. J. de Ricqlès, L. Zylberberg, & K. Padian (Eds.), Vertebrate Skeletal Histology and Paleohistology (1 ed., pp. 147-182). CRC Press. https://doi.org/https://doi.org/10.1201/9781351189590

Campione, N. E., Evans, D. C., Brown, C. M., Carrano, M. T., & Revell, L. (2014). Body mass estimation in non-avian bipeds using a theoretical conversion to quadruped stylopodial proportions. Methods in Ecology and Evolution, 5(9), 913-923. https://doi.org/10.1111/2041-210X.12226

Carrano, M. T. (1999). What, if anything, is a cursor? Categories versus continua for determining locomotor habit in mammals and dinosaurs. Journal of zoology (1987), 247(1), 29-42. https://doi.org/10.1017/S095283699900103X

Castanet, J., Francillon-Vieillot, H., Meunier, F. J., & de Ricqlès, A. J. (1993). Bone and individual aging. In B. K. Hall (Ed.), Bone (Vol. 7, pp. 245-283). CRC Press.

Castanet, J., & Naulleau, G. (1985). La squelettochronologie chez les reptiles. II. Résultats expérimentaux sur la signification des marques de croissance squelettiques chez les serpents. Remarques sur la croissance et la longévité de la vipère Aspic. Annales Des Sciences Naturelles-zoologie Et Biologie Animale, 7, 41-62.

Chinsamy, A. (1994). Dinosaur Bone Histology: Implications and Inferences. The Paleontological Society Special Publications, 7, 213-228. https://doi.org/10.1017/S2475262200009539

Crabtree, D. R. (1987). Angiosperms of the northern Rocky Mountains: Albian to Campanian (Cretaceous) megafossil floras. Annals of the Missouri Botanical Garden, 74(4), 707-747. https://doi.org/10.2307/2399448

Cubo, J., Woodward, H., Wolff, E., & Horner, J. R. (2015). First reported cases of biomechanically adaptive bone modeling in non-avian dinosaurs. PloS one, 2015(7), e0131131-e0131131. https://doi.org/10.1371/journal.pone.0131131

de Buffrénil, V., Quilhac, A., & Castanet, J. (2021). Bone Tissue Types: A Brief Account of Currently Used Categories. In V. de Buffrénil, A. J. de Ricqlès, L. Zylberberg, & K. Padian (Eds.), Vertebrate Skeletal Histology and Paleohistology (1 ed., pp. 626-644). CRC Press. https://doi.org/https://doi.org/10.1201/9781351189590

Deeming, D. C., & Birchard, G. F. (2007). Allometry of egg and hatchling mass in birds and reptiles: roles of developmental maturity, eggshell structure and phylogeny. Journal of zoology (1987), 271(1), 78-87. https://doi.org/10.1111/j.1469-7998.2006.00219.x

D'Emic, M. D., O'Connor, P. M., Sombathy, R. S., Cerda, I., Pascucci, T. R., Varricchio, D., Pol, D., Dave, A., Coria, R. A., & Curry Rogers, K. A. (2023). Developmental strategies underlying gigantism and miniaturization in non-avialan theropod dinosaurs. Science (American Association for the Advancement of Science), 379(6634), 811.

Dodson, P. (1971). Sedimentology and taphonomy of the Oldman Formation (Campanian), Dinosaur Provincial Park, Alberta (Canada). Palaeogeography, palaeoclimatology, palaeoecology, 10(1), 21-74. https://doi.org/10.1016/0031-0182(71)90044-7

Erickson, G. M. (2005). Assessing dinosaur growth patterns: a microscopic revolution. Trends in ecology & evolution (Amsterdam), 20(12), 677-684. https://doi.org/10.1016/j.tree.2005.08.012

Erickson, G. M., Makovicky, P. J., Currie, P. J., Norell, M. A., Yerby, S. A., & Brochu, C. A. (2004). Gigantism and comparative life-history parameters of tyrannosaurid dinosaurs. Nature, 430(7001), 772-775. https://doi.org/10.1038/nature02699

Erickson, G. M., Rogers, K. C., & Yerby, S. A. (2001). Dinosaurian growth patterns and rapid avian growth rates. Nature, 412(6845), 429-433. https://doi.org/10.1038/35086558

Erickson, G. M., & Tumanova, T. A. (2000). Growth curve of Psittacosaurus mongoliensis Osborn (Ceratopsia: Psittacosauridae) inferred from long bone histology. Zoological journal of the Linnean Society, 130(4), 551-566. https://doi.org/10.1006/zjls.2000.0243

Fowler, D. W., Woodward, H. N., Freedman, E. A., Larson, P. L., & Horner, J. R. (2011). Reanalysis of "Raptorex kriegsteini"; a juvenile tyrannosaurid dinosaur from Mongolia. PloS one, 2011(6), e21376-e21376. https://doi.org/10.1371/journal.pone.0021376

Francillon-Vieillot, H., de Buffrénil, V., Castanet, J., Géraudie, J., Meunier, F. J., Sire, Y., Zylberberg, L., & de Ricqlès, A. J. (1989). Microstructure and Mineralization of Vertebrate Skeletal Tissues. In J. G. Carter (Ed.), Skeletal Biomineralization: Patterns, Processes and Evolutionary Trends (pp. 471-530). American Geophysical Union.

Jerzykiewicz, T., & Sweet, A. (1987). Semi-arid floodplain as a paleoenvironmental setting of the Upper Cretaceous dinosaurs. Occasional Papers of the Tyrrell Museum of Paleontology, 3, 120-124.

Krassilov, V. A. (1981). Changes of Mesozoic vegetation and the extinction of dinosaurs. Palaeogeography, palaeoclimatology, palaeoecology, 34(3-4), 207-224. https://doi.org/10.1016/0031-0182(81)90065-1

Makovicky, P. J., & Norell, M. A. (2004). Troodontidae. In D. B. Weishampel, P. Dodson, & H. Osmóska (Eds.), The Dinosauria (2 ed., pp. 184-195): University of California Press.

Padian, K., & Lamm, E.-T. r. s. (2013). Bone histology of fossil tetrapods : advancing methods, analysis, and interpretation. University of California Press.

Persons, W. S., & Currie, P. J. (2016). An approach to scoring cursorial limb proportions in carnivorous dinosaurs and an attempt to account for allometry. Scientific reports, 6(19828), 19828-19828. https://doi.org/10.1038/srep19828

Ramezani, J., Beveridge, T. L., Rogers, R. R., Eberth, D. A., & Roberts, E. M. (2022). Calibrating the zenith of dinosaur diversity in the Campanian of the Western Interior Basin by CA-ID-TIMS U–Pb geochronology. Scientific reports, 12(1), 16026. https://doi.org/10.1038/s41598-022-19896-w

Varricchio, D. J. (1995). Taphonomy of Jack's Birthday Site, a diverse dinosaur bonebed from the Upper Cretaceous Two Medicine Formation of Montana. Palaeogeography, palaeoclimatology, palaeoecology, 114(2-4), 297-323. https://doi.org/10.1016/0031 0182(94)00084-L

Varricchio, D. J. (1997). Troodontidae. In P. J. Currie & K. Padian (Eds.), The Encyclopedia of Dinosaurs (pp. 749-754). San Diego: Academic Press.

Varricchio, D. J., Jackson, F., Borkowski, J. J., & Horner, J. R. (1997). Nest and egg clutches of the dinosaur Troodon formosus and the evolution of avian reproductive traits. Nature (London), 385(6613), 247-250. https://doi.org/10.1038/385247a0

Varricchio, D. J., Moore, J. R., Erickson, G. M., Norell, M. A., Jackson, F. D., & Borkowski, J. J. (2008). Avian paternal care had dinosaur origin. Science (American Association for the Advancement of Science), 322(5909), 1826-1828. https://doi.org/10.1126/science.1163245

Varricchio, D. J., Jackson, F. D., Jackson, R. A., & Zelenitsky, D. K. (2013). Porosity and water vapor conductance of two Troodon formosus eggs; an assessment of incubation strategy in a maniraptoran dinosaur. Paleobiology, 39(2), 278-296. https://doi.org/10.1666/11042

Wolfe, J. A., & Upchurch, G. R. (1986). Vegetation, climatic and floral changes at the Cretaceous-Tertiary boundary. Nature (London), 324(6093), 148-152. https://doi.org/10.1038/324148a0

CHAPTER THREE

HIND LIMB SKELETAL ONTOGENY OF THE EMU AND A COMPARISON TO THE TROODONTID THEROPOD *TROODON FORMOSUS*

Contribution of Authors and Co-Authors

Manuscript in Chapter 3

Author: Harris R. Boekenheide

Contributions: Designed project and drafted manuscript, gathered and interpreted data, created figures.

Co-Author: David J. Varricchio

Contributions: Editing, provided direction, advice, expertise

Co-Author: Matthew T. Carrano

Contributions: Editing, provided advice and expertise

Manuscript Information

Harris R. Boekenheide, David J. Varricchio, Matthew T. Carrano

Journal of Vertebrate Paleontology

Status of Manuscript:

_x_ Prepared for submission to a peer-reviewed journal

____ Officially submitted to a peer-reviewed journal

____ Accepted by a peer-reviewed journal

____ Published in a peer-reviewed journal

Hind limb skeletal ontogeny of the emu and a comparison to the troodontid theropod *Troodon formosus*

HARRIS R. BOEKENHEIDE[*,1], DAVID J. VARRICCHIO[2], MATTHEW T. CARRANO[3]

[1]Department of Earth Sciences, Montana State University, Bozeman, Montana 59717, U.S.A., hrboekenheide@gmail.com;

[2]Department of Earth Sciences, Montana State University, Bozeman, Montana, 59717, U.S.A., djv@montana.edu;

[3] Paleobiology Department, Smithsonian National Museum of Natural History, Washington, D.C., 20560, U.S.A., carranom@si.edu

*Corresponding author

Abstract

ABSTRACT— Modern avians have undergone an astounding number of novel evolutionary developments in the time since diverging from the non-avian theropod lineage, such as the extensive loss or fusion of skeletal elements, the drastic shift in gait and pelvic limb bone functionality, the acquisition of an edentulous beak, and of course, powered flight. Despite these differences, as the closest extant relatives to theropod dinosaurs, we often turn to them to better understand their extinct relatives. By examining emus as a potential ontogenetic and locomotive model for the Campanian theropod *Troodon formosus*, better understand the applicability of cursorial avians as modern analogues for non-avian theropods. We observed linear and highly-isometric scaling in the emus relative to *Troodon* and judged it to be unfit as a modern analogue.

INTRODUCTION

Emus

Dromaius novaehollandiae, more commonly known as the emu, is a species of ratite native to Australia. It is one of the largest extant avian species in the world and is closely related to similarly large, flightless birds such as ostriches, cassowaries, and rheas. We then used the hind limb bones of *Dromaius* as a model and point of comparison for the Campanian troodontid theropod, *Troodon formosus.* By using emus as a modern analogue, we hope to gain a better understanding of how effective modern ratites are as an ontogenetic analogue for non-avian theropods, as well as the changes undergone in the dimensions of theropod pelvic limb bones between the Late Cretaceous and Quaternary periods.

Cursoriality

Cursoriality is generally defined as the energy efficiency of locomotion in terrestrial organisms, or the ease with which an individual moves from one location to another. Species with high degrees of cursoriality are able to move long distances with minimal energy expenditure and are therefore described as “cursorial.” Those that expend relatively large amounts of energy to travel the same distance are known as “graviportal”. The two are not distinct categories, but rather the endpoints of a spectrum (Carrano, 1999). Cursoriality is not strictly about running speed. Some extant megafauna, such as the bison, have been scored as aligning more on the graviportal side of the cursoriality spectrum, despite being able to maintain a maximum running speed of 55 kph (35 mph) for a full hour (Carrano, 1999). While the exact definition of cursoriality is somewhat nebulous, the term is often associated with slender, long-limbed organisms. Conversely, stout, heavy organisms are often graviportal. High degrees of

cursoriality within dinosauria are mainly constrained to carnivorous theropods, as cursorial morphology in large herbivores, “frequently relates more to endurance and the ability to continuously forage across expansive home ranges” (Persons & Currie, 2016). Little has been done on how theropod cursoriality changes with ontogeny, likely due to a lack of associated juvenile material. The current literature shows that there have been several studies on theropod cursoriality in the past, but they have mostly focused on the cursorial differences between theropod clades, comparing the athleticism of distant relatives to one another. Comparisons of Troodontidae to its sister group, Dromaeosauridae, by Fowler et al. (2011), indicate a divergence in the predatory ecologies. Namely, the proportions of their feet and the articular facets of their phalanges indicate a partitioning of ecological niches. Troodontids acquired a greater degree of cursoriality that would have been used to chase down prey, whereas dromaeosaurids sacrificed speed to increase grasping strength, a development more suitable for an ambush predator.

Ontogenetic Changes in Cursoriality— Ontogenetic changes in cursoriality are known to play significant roles in extant taxa. Komodo dragons, for instance, switch to an entirely separate ecological niche as they mature (Purwandana et al., 2016). Lightweight, cursorial juveniles tend to be mainly arboreal. As they grow older and take on greater amounts of mass relative to their size, they eventually become unable to scale trees and must hunt for food on the ground. Modern avians also are known to be subject to ontogenetic changes in cursoriality. Research by Muir et al. (1996), found that extant precocial birds undergo noticeable cursorial change within the first two weeks of life; however, this is not so much the result of changing limb proportions as it is a chick learning to walk more efficiently. A day-old chick will adopt the same style of running as a chick two weeks in age, such cursorial changes only apply to a chick when it is walking.

While extant mammals exhibit a wide variety of cursorial values, as well as ontogenetic changes in cursoriality, previous studies have concluded that it is not necessarily achieved in the same manner as extinct non-avian and avian theropods. Research by Day and Jayne (2007), involving nine species of felids ranging from domestic cats to cheetahs, found that feline taxa have remarkably similar appendicular skeletal proportions, and that differences in cursoriality are due more to differing limb posture.

METHODS

Institutional Abbreviations— **MOR**, Museum of the Rockies, Bozeman, U.S.A.

Anatomical Abbreviations— **MT**, metatarsal; **TMT**, tarsometatarsus.

Emu Background

Emu carcasses of a multitude of ages were acquired from Montana Emu Ranch Co. in Kalispell, Montana. After hatching, the emus of Montana Emu Ranch Co. are kept in 2’x3’ or 2’x4’ brooder boxes for five days, after which they are moved to a second brooder box measuring 5’x6’. Weather permitting, they are let out into a 15’x3’ indoor/outdoor pen in the daytime. At three months of age, the emus are moved into grow-out pens, ranging from about ½ to 1 square acre. Emus are fed via free-choice feeding. The dietary content of the feed of most emus varies by age. The sole exception to this diet is individuals raised specifically for breeding. The breeder diet consists of 20.0% crude protein, 4.0% fat, and 7.0% fiber (P. Collins, personal communication, September 2, 2021).

Emu Preparation

One leg of each emu carcass was severed at the femoroacetabular joint, after which it was cleaned of remaining soft tissue by dermestid beetles. The remaining bones were soaked for one week in water, followed by an additional week in a solution consisting of approximately 2.5 tablespoons terg-a-zyme per gallon of water.

Calculating Emu Body Mass

Anderson et al. (1985), found that traditionally-accepted equations for calculating body mass based on femoral circumference tend to give inaccurate results when applied to ratites. They attributed this to potentially being a result of the horizontally-oriented femur. This phenomenon was observed to occur even in more recent equations for the estimation of body mass, such as Campione et al. (2014). Therefore, a separate equation penned by Anderson et al. has been used to estimate the body mass of the emus, using femoral circumference (C_f) to estimate weight (W) (See Appendix B for full list of emu hind limb measurements).

Equation 6:

$$W = (1.08 * C_f^{2.28 \pm 0.1})$$

Records noting the ages of the emus provided for this study were sporadic, and as a result many of the emus' ages were approximated using comparisons to those whose ages were provided. As the largest emu in the dataset was among those without ages provided, it was given an age estimate of 248 days based on a previous study on emu body mass by Blake and Hess (2004). The body mass of *Troodon* was estimated using Campione et al. (2014) and D'Emic et al. (2023).

Ontogenetic Scaling

Traditionally, estimating the body masses of individuals of various ontogenetic stages for extinct taxa would make use of an equation by Erickson and Tumanova (2000) in which the femoral length and body mass of the largest individual are found, and then the femoral lengths of juvenile femora are scaled isometrically to the 0.33 power. The question of testing Erickson & Tumanova's methodology was only taken into consideration after one leg of each emu had already been severed and fully prepared. Therefore, we weighed the now one-legged emus, then severed the remaining leg and added its mass to that of the one-legged emu to estimate full body mass. However, application of the Erickson & Tumanova methodology to calculate body mass produced results that were less accurate than Anderson et al., which produced body mass estimates very close to what was expected. Since we were attempting body mass estimates for *Troodon* as well, we decided to test it against the methodology from Campione et al. (2014) as well. In every test, incorporating Erickson and Tumanova's ontogenetic scaling exponent into the methodology of Campione et al. decreased the accuracy of the results. Looking deeper into Erickson and Tumanova (2000) revealed that their scaling exponent was created based on the phylogenetic bracketing of Archosauria. One half of this bracket, meant to represent avian taxa, was in reference to a 1990 study by Carrier and Leon about *Larus californicus*, the California gull. Looks into the existing literature showed no evidence of any actualistic testing verifying the applicability of Erickson and Tumanova's (2000) scaling exponent. Therefore, it was decided that Erickson and Tumanova's ontogenetic scaling exponent would not be included in the final results.

Within-Element Measurements

Measurements were also taken in order to determine how proportions change within individual bones. The anteroposterior and mediolateral lengths of bones were taken for the proximal and distal ends, as well as the shaft (Appendix C).

Emu and *Troodon* Hind Limb Growth

Several growth curves were constructed in Microsoft Excel, comparing the growth of *Troodon* and *Dromaius.* These growth curves plot the relative lengths of the cursorial limb bones, changes in body mass, and within-element allometric changes.

The cnemial crest of the emu fuses to the tibiotarsus with age, adding to its length. However, it is unlikely that the crest impacts the full length of the cursorial limb, given that the crest cradles the distal articular facets of the femur. Therefore, it was decided that measurements taken of the emu tibiotarsi would exclude the length added by the cnemial crest.

Calculating Cursoriality

The cursorial abilities of *Troodon* were scored against one another using the methodology of Persons and Currie (2016), in which bone allometry and body size are taken into account. In this equation, the expected lower leg length of a hypothetical average individual (l) is calculated using femoral length, (f).

Equation 7:

$$l=4.178f^{0.8371}$$

Individuals are then scored as being more or less cursorial than the hypothetical individual by comparing the actual lower-leg length of an individual (the sum length of the tibia

and third metatarsal in non-avian theropods) to the expected lower-leg length (l) that had been calculated.

As this methodology had been designed specifically for carnivorous non-avian theropods, a different approach by Jones et al. (2000) was used to compare the cursorial abilities of *Troodon* and the emu, as it had been used in their study to judge the cursoriality of both avian and non-avian theropods by comparing their effective leg lengths to trunk lengths (EL/TL). The bones that contribute to effective leg length differ between non-avian and avian theropods. In the *Troodon,* it included the lengths of the femur, tibia, and third metatarsal. With the femur's reduced role in locomotion, Jones et al. (2000) considered the effective leg length of avian theropods to consist only of the tibiotarsus and tarsometatarsus.

Body mass was estimated in *T. formosus* using the methodology of Campione et al. (2014). Emu body mass was estimated using a species-specific equation by Anderson et al. (1985).

Metatarsal Proxies

Due to extreme mediolateral constraint of the third metatarsal in *Troodon,* the majority of the fossils from the dataset only included isolated distal ends that tapered to a point proximally. A single well-preserved foot of *T. formosus* has been found (MOR 748), which also includes MTs II through IV. It was decided that complete second and fourth metatarsals may be used to estimate the length of MT III in order to work around the lack of complete third MTs in other specimens. Observation of emu TMTs showed only minor degrees of individual variation among metatarsal proportions, with no clear changes resulting from ontogeny. Therefore, it was determined that in cases in which a third metatarsal may be missing or incomplete, the relative

proportions of the metatarsals of MOR 748 could be used as a standard to estimate metatarsal length.

RESULTS

Emu Femur

The dimensions of the femur tended to scale isometrically through ontogeny [Fig. 3.1]. The sole exception to this isometric scaling seems to be femora that were approximately 150 – 180 mm in length, at which point length and circumference appear not to grow simultaneously. Instead, it would appear that length quickly increases, with relatively minor changes in circumference. Then, the femur is thickened during a temporary cessation in the bone's lengthening. Following this single deviation, the femora returned to their original isometric scaling. Compared to *Troodon*, the femur of the emu is far more stout.

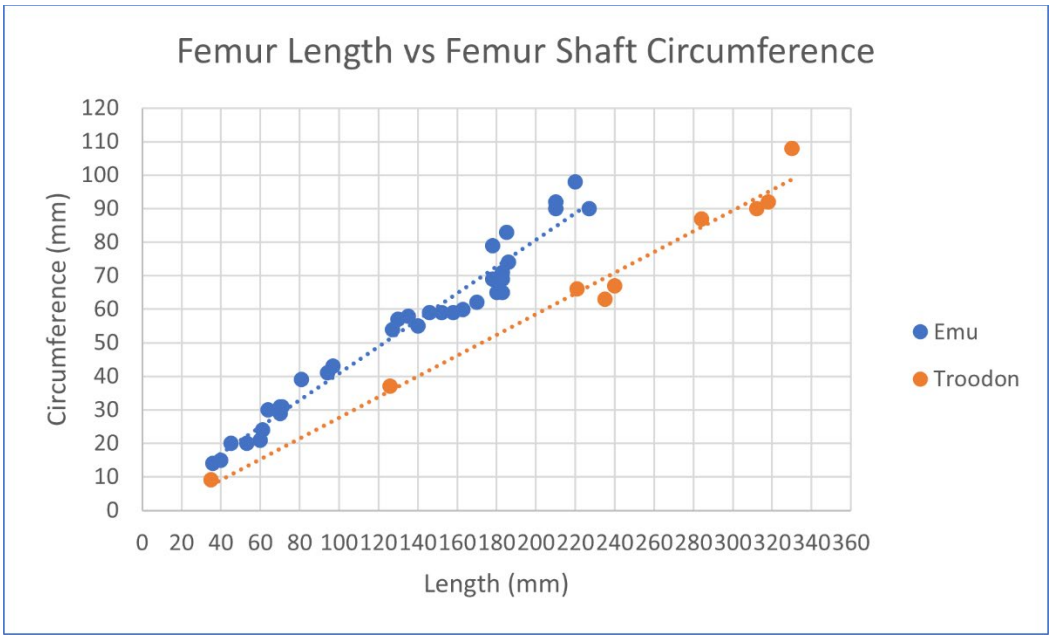

FIGURE 3.1. *Troodon* and emu femoral length vs. femoral circumference [planned for 2/3 page width].

Emu Tibia

While the femora were relatively thick in the emu, the opposite was shown to be true in the tibia, with the tibiotarsi of the emu possessing far smaller minimum shaft circumferences relative to length. However, much like the femur, scaling observed in the tibiotarsus of the emu was largely isometric, with the minimum shaft circumference remaining about 10% of the bone's length throughout ontogeny [Fig. 3.2].

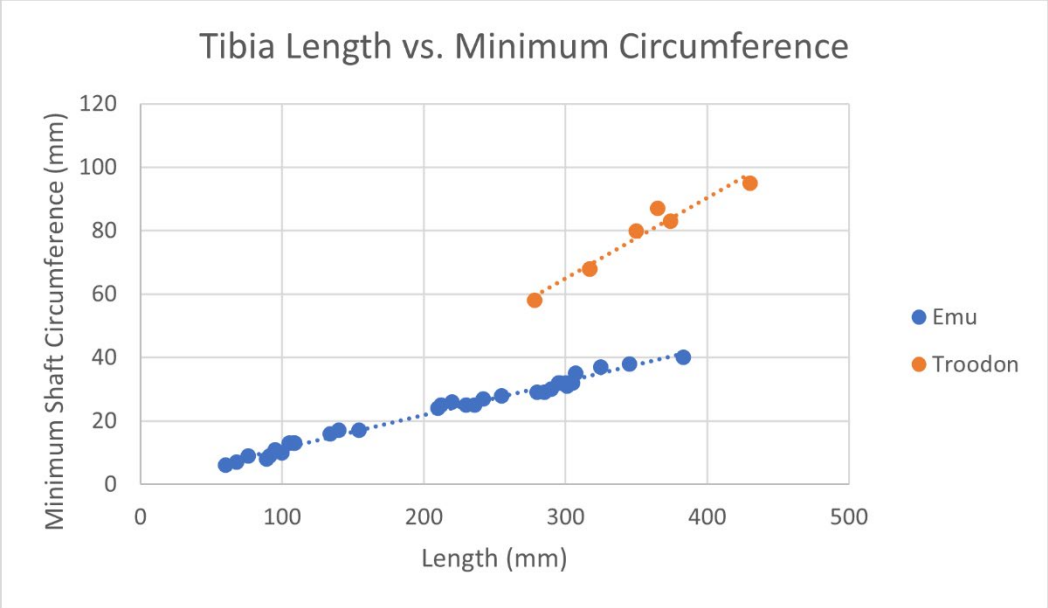

FIGURE 3.2. *Troodon* and emu tibial length vs. minimal circumference [planned for 2/3 page width].

Emu Metatarsals

Not much could be gleaned from comparisons of *Troodon* metatarsals to the tarsometatarsi of the emu (See Appendix C). Metatarsals II – IV are thoroughly fused in the emu, with only their distalmost portions spread out enough to distinguish individually. The dimensions of the tarsometatarsal shaft changes a great deal along its length, decreasing distally. Like the rest of the elements observed in the emu, the range of minimum to maximum shaft dimensions is largely isometric through ontogeny, with the maximum anteroposterior and mediolateral dimensions always being approximately double that of the minimum anteroposterior and mediolateral dimensions, respectively [Fig. 3.3]. Proportions between the lengths of each metatarsal varied only slightly between individuals, with no observed correlation to ontogeny.

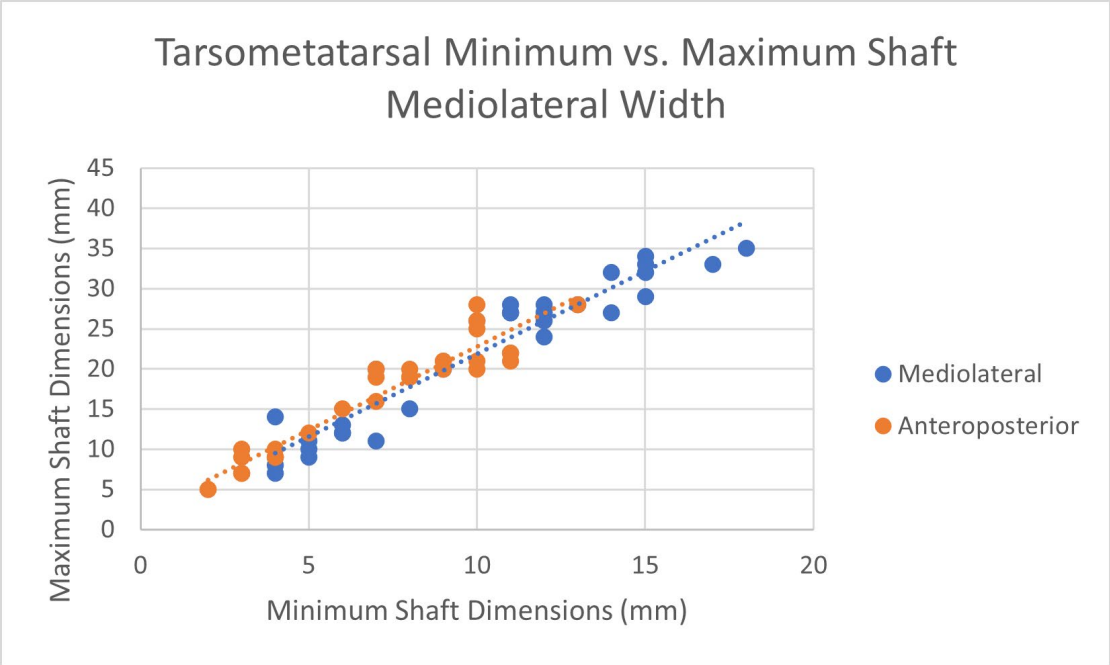

FIGURE 3.3. Minimum versus maximum width of the emu tarsometatarsus [planned for 2/3 page width].

Emu Hind Limb Scaling

Scaling between the hind limb bones of the emu was found to be strongly isometric, similar to the scaling observed within the individual bones [Fig. 3.4]. Both the relative proportions between and within the hind limb elements of the emu were observed to scale linearly and oftentimes isometrically.

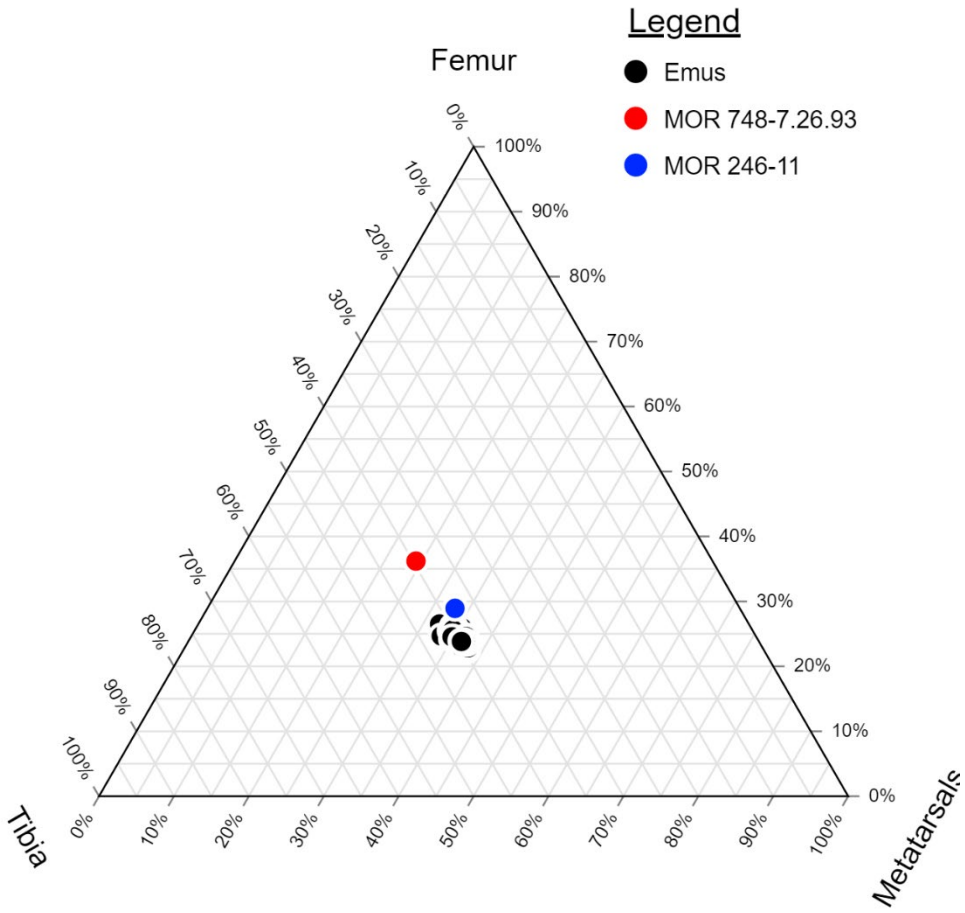

FIGURE 3.4. Ternary diagram depicting proportionality of hind limb elements in the emu and *Troodon* [planned for 2/3 page width].

***Troodon* Femur**

Conversely to the emu's use of a short, thick femur, *Troodon* was able to support a greater body mass with a proportionally thinner femur. However, the scaling of the femoral length versus femoral circumference is shown to be largely isometric, much like the emu [Fig. 3.2].

***Troodon* Tibia**

There appeared to be some minor allometry in the scaling present with the bone thickening at a slightly faster rate than it lengthened at [Fig. 3.2]. The only other observable

pattern in the ontogenetic scaling of the *Troodon* tibia was possible allometric scaling present in the distal dimensions, with mediolateral growth occurring at far faster rates than anteroposterior growth (see Appendix C).

Troodon Metatarsals

A set of associated second, third, and fourth metatarsals have only been found in a single *Troodon* specimen, MOR 748. Additionally, among the remaining isolated bones, the longest and arguably most informative of these metatarsals is consistently broken due to the extreme mediolateral constraint of the third metatarsal present in the arctometatarsalian pes. Therefore, the only comparisons that could be made between the emu tarsometatarsus and the metatarsals of *Troodon* are the dimensions of the distal epiphyses. The results showed the distal metatarsals of the emu being far more broad and flat relative to *Troodon*. Whereas the distal dimensions of *Troodon* metatarsals were often nearly equal, with the anteroposterior diameter being only slightly greater than the mediolateral diameter. In the emu, however, the mediolateral diameter was the greater of the two.

Troodon Hind Limb Scaling

As we possessed both embryonic and adult *Troodon* individuals with all three cursorial limb bones (femur, tibia, and third metatarsal) either present or able to be approximated, we decided to compare the proportions of each bone to one another to see how they change through ontogeny. For the sake of comparison, the same was done for the smallest and largest emus included in the dataset. As noted previously, scaling in the emu was strongly isometric. However, significant degrees of non-linear and allometric scaling patterns were observed in *Troodon*. In *Troodon*, bone length scales the most proximally and decreases distally. The adult

Troodon femur grew to approximately 9.1 times the length of the embryonic femur, while the metatarsals only grew to be 5.4 times their original size. Scaling of the tibia fell in the middle at 7.6 times the embryonic size.

Troodon vs. Emu Cursoriality

The differing locomotive biomechanics between *Troodon* and emus make a direct comparison of their cursorial abilities somewhat tenuous. However, use of the equation by Jones et al. (2000), we were able to determine that the largest emu included in the dataset had an effective leg length 1.13 times its trunk length. Meanwhile, the adult *Troodon* MOR 748 possessed an effective leg length 1.47 times the length of its trunk. Therefore, it can be determined that the adult emu that was sampled is less cursorial than the adult *Troodon*. As stated previously, comparisons of the cursorial abilities of taxa with such different locomotive styles remains questionable and should not be taken at face value. Despite the horizontal femoral posture and knee-based locomotion typical of extant birds (Carrano 1998), the femur still plays a role in emu locomotion, with a range of motion of approximately 50° (Abourachid & Renous, 2000). It is likely that extant equines may prove to be a better modern analogue for non-avian theropod locomotion, as suggested by Carrano (1998).

Troodon Cursoriality through Ontogeny

As a result of the disarticulation of the elements found at Jack's Birthday Site, cursorial values for the majority of *Troodon* individuals were unable to be determined. However, two individuals from other locations were complete enough for cursoriality to be calculated. Both individuals possessed a femur, a tibia, and an associated third (or fourth) metatarsal. One such specimen, MOR 246-11, is a nearly fully developed embryo. Proportional changes between

bones are unlikely to occur so late in embryonic development, meaning the embryo could act as proxy for a hatchling. The other individual, MOR 748, represents a somatically mature adult. Persons and Currie (2016) had previously calculated the cursorial value of MOR 748, using an equation that accounts for allometric differences between species of similar sizes. They gave it a score of +7.6, suggesting that *Troodon* is relatively cursorial. This study obtained a slightly higher value with +7.9 after using the same equation. Meanwhile, MOR 246-11 was scored at +7.3. The difference between the cursorial values found between the hatchling and adult are small enough to be potentially attributable to individual variation.

DISCUSSION

The ontogenetic scaling observed in emu, both between elements and within elements, was consistently linear and often isometric (Table 5). The hind limb scaling being more allometric in *Troodon* and isometric in emu coincides with our current understanding of theropods. Carnivorous theropods tend to possess a degree of allometric scaling, whereas herbivorous theropods scale much more isometrically through ontogeny (Lu et al., 2013). Comparing *Troodon* to the emu showed the latter as possessing a shortened and thickened femur, a longer and more slender tibia, and relatively flattened and mediolaterally-spread distal metatarsals.

Graph	Emu	Emu R2	*Troodon*	*Troodon* R2
Femur Circ. / Femur Length	y=0.3965x+1.2318	0.9574	y=0.3204x-8.383	0.8824
Femur Prox. ML / Prox. AP	y=0.9953x-1.5452	0.8974	y=0.9835x+8.9489	0.8478
Femur Shaft ML / Shaft AP	y=0.9527x+0.917	0.8752	y=1.1214x-2.581	0.9709
Femur Prox. AP / Distal AP	y=1.1832x-2.2464	0.9703	y=0.8929x-3.0357	0.9893
Femur Prox. ML / Distal ML	y=1.1911x+1.8981	0.958	y=1.0123x-4.705	0.9057
Femur Distal ML / Distal AP	y=1.0583x+0.4124	0.9884	y=0.8309x+17.635	0.9462
Tibia Min. Circ. / Tibia Length	y=0.1059x+0.698	0.9862	y=0.2547x-11.452	0.9489
Tibia Prox. ML / Prox. AP	y=0.5481x+1.7942	0.9361	y=0.3741x+20.03	0.0792
Tibia Shaft ML / Shaft AP	y=1.0121x+0.5593	0.9416	y=1.1852x-0.027	0.942
Tibia Prox. AP / Distal AP	y=0.2646x+2.4529	0.8668	y=0.0514x+14.448	0.2087
Tibia Prox. ML / Distal ML	y=0.9835x+5.7558	0.9334	y=0.4794x+31.974	0.7391
Tibia Distal ML / Distal AP	y=1.973x+3.4171	0.944	y=3.5729x-10.452	0.8363
MTIII Distal ML / Distal AP	y=1.1079x+0.6722	0.9666	y=x-4	0.8
MTIV Distal ML / Distal AP	y=1.5578x+1.9918	0.9585	0.8511x-1.8255	0.9644
Tibia Length / Femur Length	y=1.0219x+0.3825	0.9952	y=0.917x+0.5684	1
Femur Length / MTIII Length	y=0.9045x+0.1077	0.9925	y=1.3117x-1.27	1
MTIII Length / Tibia Length	y=0.9282x+0.4727	0.9961	y=0.8314x+0.4957	1

TABLE 5. Linear regression analysis on Emu and *Troodon* hind limb proportions [planned for 2/3 page width].

CONCLUSION

Observation of how the hind limb scale with ontogeny in *Troodon formosus* and the extant emu reinforce the notion that cursorial birds are insufficient modern ontogenetic or locomotive analogues for non-avian theropods (Carrano, 1998; Grossi et al., 2019). The isometric scaling in emus

makes it a similarly poor analogue for examining the ontogeny of the allometrically-scaling *Troodon*.

Comparison of ontogenetic scaling in the hind limb bones of *Troodon* and emu bones have provided further insight into the theropod evolutionary transition to the avian lineage. Many

of the differences present appear to be related to the shift in the positioning and function of the femur. This change to a more horizontally-oriented femur has been considered significant for the acquisition of behaviors that would eventually lead to the flight (Heers & Dial, 2012), such as launching and landing (Earls, 2000), flap-running (Dial et al., 2011; Dial, 2003, Dial et al., 2008), and tree-climbing (Zhang et al., 2002).

Troodontids have been cited previously as being one of the most cursorial theropod taxa (Carrano, 1999; Persons & Currie, 2016). From this study, it seems likely that this cursoriality remains consistent throughout ontogeny. Additionally, comparison of *Troodon* cursoriality to that of the modern emu, *Dromaius novaehollandiae* has put its abilities into better perspective. It appears that *Troodon formosus* was better suited for energy-efficient locomotion than even one of the most cursorial extant avians.

ACKNOWLEDGEMENTS

I would like to thank Don and Penni Collins of Montana Emu Ranch Co. for the generous donation of emus; Eric Metz for instruction on modern bone preparation; my graduate cohort for being such an effective escape from work; to Heath Caldwell and Emilio Bedolla for taking over emu duty and putting an end to the complaints about the smell in the CVA lab; to Dr. John Scannella and Museum of the Rockies for the loan of Troodon specimens; the Blackfeet Nation, the families of Lewis Carroll, Vernon Carroll, Huey Monroe, MOR inc., The Nature Conservancy, and the Peebles families for permission to excavate and collect the fossils from their land; the National Science Foundation for funding John Horner's field work when these specimens were collected; and Montana State University's Department of Earth Sciences. Finally, I would like to thank my parents for their tireless support and understanding.

LITERATURE CITED

Abourachid, A., & Renous, S. (2000). Bipedal locomotion in ratites (Paleognatiform): examples of cursorial birds. Ibis (London, England), 142(4), 538-549. https://doi.org/10.1111/j.1474-919X.2000.tb04455.x

Anderson, J. F., Hall-Martin, A., & Russell, D. A. (1985). Long-bone circumference and weight in mammals, birds and dinosaurs. Journal of Zoology, 207(1), 53-61.

Blake, J. P., & Hess, J. B. (2004). Effect of Protein on Growth and Carcass Yield of Emu. International journal of poultry science, 3(3), 211-214. https://doi.org/10.3923/ijps.2004.211.214

Campione, N. E., Evans, D. C., Brown, C. M., Carrano, M. T., & Revell, L. (2014). Body mass estimation in non-avian bipeds using a theoretical conversion to quadruped stylopodial proportions. Methods in Ecology and Evolution, 5(9), 913-923. https://doi.org/10.1111/2041-210X.12226

Carrano, M. T. (1998). Locomotion in non-avian dinosaurs: integrating data from hindlimb kinematics, in vivo strains, and bone morphology. Paleobiology, 24(4), 450-469. https://doi.org/10.1017/S0094837300020108

Carrano, M. T. (1999). What, if anything, is a cursor? Categories versus continua for determining locomotor habit in mammals and dinosaurs. Journal of zoology (1987), 247(1), 29-42. https://doi.org/10.1017/S095283699900103X

Carrier, D., & Leon, L. R. (1990). Skeletal growth and function in the California gull (Larus californicus). Journal of zoology (1987), 222(3), 375-389. https://doi.org/10.1111/j.1469 7998.1990.tb04039.x

Day, L. M., & Jayne, B. C. (2007). Interspecific scaling of the morphology and posture of the limbs during the locomotion of cats (Felidae). Journal of experimental biology, 210(Pt 4), 642-654. https://doi.org/10.1242/jeb.02703

Deeming, D. C., & Birchard, G. F. (2007). Allometry of egg and hatchling mass in birds and reptiles: roles of developmental maturity, eggshell structure and phylogeny. Journal of zoology (1987), 271(1), 78-87. https://doi.org/10.1111/j.1469-7998.2006.00219.x

D'Emic, M. D., O'Connor, P. M., Sombathy, R. S., Cerda, I., Pascucci, T. R., Varricchio, D., Pol, D., Dave, A., Coria, R. A., & Curry Rogers, K. A. (2023). Developmental strategies underlying gigantism and miniaturization in non-avialan theropod dinosaurs. Science (American Association for the Advancement of Science), 379(6634), 811.

Dial, K. P. (2003). Wing-Assisted Incline Running and the Evolution of Flight. Science (American Association for the Advancement of Science), 299(5605), 402-404. https://doi.org/10.1126/science.1078237

Dial, K. P., Jackson, B. E., & Segre, P. (2008). A fundamental avian wing-stroke provides a new perspective on the evolution of flight. Nature, 451(7181), 985-989. https://doi.org/10.1038/nature06517

Dial, K. P., Randall, R. J., & Dial, T. R. (2006). What Use Is Half a Wing in the Ecology and Evolution of Birds? Bioscience, 56(5), 437-445. https://doi.org/10.1641/0006 3568(2006)056[0437:WUIHAW]2.0.CO;2

Earls, K. D. (2000). Kinematics and mechanics of ground take-off in the starling Sturnis vulgaris and the quail Coturnix coturnix. Journal of experimental biology, 203(Pt 4), 725-739. https://doi.org/10.1242/jeb.203.4.725

Erickson, G. M., & Tumanova, T. A. (2000). Growth curve of Psittacosaurus mongoliensis Osborn (Ceratopsia: Psittacosauridae) inferred from long bone histology. Zoological journal of the Linnean Society, 130(4), 551-566. https://doi.org/10.1006/zjls.2000.0243

Fowler, D. W., Woodward, H. N., Freedman, E. A., Larson, P. L., & Horner, J. R. (2011). Reanalysis of "Raptorex kriegsteini"; a juvenile tyrannosaurid dinosaur from Mongolia. PloS one, 2011(6), e21376-e21376. https://doi.org/10.1371/journal.pone.0021376

Grossi, B., Loncomilla, P., Canals, M., & Ruiz-Del-Solar, J. (2019). Are Cursorial Birds Good Kinematic Models of Non-Avian Theropods? International journal of morphology, 37(2), 620-625. https://doi.org/10.4067/S0717-95022019000200620

Heers, A. M., & Dial, K. P. (2012). From extant to extinct: locomotor ontogeny and the evolution of avian flight. Trends in ecology & evolution (Amsterdam), 27(5), 296-305. https://doi.org/10.1016/j.tree.2011.12.003 https://doi.org/10.1002/jmor.1052090107

Jones, T. D., Farlow, J. O., Ruben, J. A., Henderson, D. M., & Hillenius, W. J. (2000). Cursoriality in bipedal archosaurs. Nature (London), 406(6797), 716-718. https://doi.org/10.1038/35021041

Lu, J., Currie, P. J., Xu, L., Zhang, X., Pu, H., & Jia, S. (2013). Chicken-sized oviraptorid dinosaurs from central China and their ontogenetic implications. Die Naturwissenschaften, 100(2), 165-175. https://doi.org/10.1007/s00114-012-1007-0

Muir, G. D., Gosline, J. M., & Steeves, J. D. (1996). Ontogeny of bipedal locomotion: walking and running in the chick. The Journal of physiology, 493(Pt 2), 589-601. https://doi.org/10.1113/jphysiol.1996.sp021406

Persons, W. S., & Currie, P. J. (2016). An approach to scoring cursorial limb proportions in carnivorous dinosaurs and an attempt to account for allometry. Scientific reports, 6(19828), 19828-19828. https://doi.org/10.1038/srep19828

Phillips, M. J., Gibb, G. C., Crimp, E. A., & Penny, D. (2009). Tinamous and Moa Flock Together: Mitochondrial Genome Sequence Analysis Reveals Independent Losses of Flight among Ratites. Systematic Biology, 59(1), 90-107. https://doi.org/10.1093/sysbio/syp079

Purwandana, D., Ariefiandy, A., Imansyah, M. J., Seno, A., Ciofi, C., Letnic, M., & Jessop, T. S. (2016). Ecological allometries and niche use dynamics across Komodo dragon ontogeny. Die Naturwissenschaften, 103(3-4), 27. https://doi.org/10.1007/s00114-016-1351-6

Suganya, G., Leela, V., Paramasivam, A., Richard Jagatheesan, P. (2017). Growth performance of emu chicks reared under intensive farming conditions. International Journal of Science, Environment, and Technology, 6(6), 3367-3371.

Varricchio, D. J., Jackson, F. D., Jackson, R. A., & Zelenitsky, D. K. (2013). Porosity and water vapor conductance of two Troodon formosus eggs; an assessment of incubation strategy in a maniraptoran dinosaur. Paleobiology, 39(2), 278-296. https://doi.org/10.1666/11042

Zhang, F., Zhou, Z., Xu, X., & Wang, X. (2002). A juvenile coelurosaurian theropod from China indicates arboreal habits. Die Naturwissenschaften, 89(9), 394-398. https://doi.org/10.1007/s00114-002-0353-8

CHAPTER FOUR

CONCLUSIONS

The observation and examination of the hind limb bones of *Troodon formosus* has provided a wealth of new data and expanded our understanding of this fascinating species. This includes information on growth rates, locomotive strategies, and the mechanical innovations involved in the evolutionary transition from non-avian to avian theropods.

Histologic analysis of femoral and tibial skeletal growth markers suggests highly variable growth, which has in turn increased the estimated body mass of *Troodon* from 45 kg - 50 kg to nearly 75 kg. Given the apparent homogeny of growth rates observed in juvenile individuals, we interpret the eventual divergent growth as evidence for sexually dimorphic sizes in *Troodon*, though we can not entirely discount the possibility of it being the result of individual variation.

Ontogenetic scaling in the hind limb bones of the emu was shown to be strongly isometric, whereas the proportions between elements was allometric in *Troodon.* Additionally, comparison of hind limb proportions and dimensions between *Troodon* and the emu further highlight the evolutionary changes undergone across the non-avian to avian theropod lineage. Even in avians that have secondarily lost the ability, the femur is still structured and positioned to accommodate behaviors associated with flight. Instead of a reversal of femoral evolution, the tibiotarsus and tarsometatarsus have further developed over time and diverged from the condition found in non-avian theropods to allow for greater degrees of cursoriality.

Finally, comparison of the cursorial capabilities of embryonic remains to a sexually-mature *Troodon* show no significant change through ontogeny. However, comparison to the

extant emu evidence greater cursoriality in *Troodon*, creating a better perspective on just how well-adapted this species was for energy-efficient movement.

REFERENCES CITED

Abourachid, A., & Renous, S. (2000). Bipedal locomotion in ratites (Paleognatiform): examples of cursorial birds. Ibis (London, England), 142(4), 538-549. https://doi.org/10.1111/j.1474-919X.2000.tb04455.x

Anderson, J. F., Hall-Martin, A., & Russell, D. A. (1985). Long-bone circumference and weight in mammals, birds and dinosaurs. Journal of Zoology, 207(1), 53-61.

Barta, D. E., Griffin, C. T., & Norell, M. A. (2022). Osteohistology of a Triassic dinosaur population reveals highly variable growth trajectories typified early dinosaur ontogeny. Scientific reports, 12(1), 17321-17321. https://doi.org/10.1038/s41598-022-22216-x

Blake, J. P., & Hess, J. B. (2004). Effect of Protein on Growth and Carcass Yield of Emu. International journal of poultry science, 3(3), 211-214. https://doi.org/10.3923/ijps.2004.211.214

Brinkman, D. B. (1990). Paleoecology of the Judith River Formation (Campanian) of Dinosaur Provincial Park, Alberta, Canada : evidence from vertebrate microfossil localities. Palaeogeography, palaeoclimatology, palaeoecology, 78(1-2), 37-54.

Campione, N. E., Evans, D. C., Brown, C. M., Carrano, M. T., & Revell, L. (2014). Body mass estimation in non-avian bipeds using a theoretical conversion to quadruped stylopodial proportions. Methods in Ecology and Evolution, 5(9), 913-923. https://doi.org/10.1111/2041-210X.12226

Carrano, M. T. (1998). Locomotion in non-avian dinosaurs: integrating data from hindlimb kinematics, in vivo strains, and bone morphology. Paleobiology, 24(4), 450-469. https://doi.org/10.1017/S0094837300020108

Carrano, M. T. (1999). What, if anything, is a cursor? Categories versus continua for determining locomotor habit in mammals and dinosaurs. Journal of zoology (1987), 247(1), 29-42. https://doi.org/10.1017/S095283699900103X

Carrier, D., & Leon, L. R. (1990). Skeletal growth and function in the California gull (Larus californicus). Journal of zoology (1987), 222(3), 375-389. https://doi.org/10.1111/j.14697998.1990.tb04039.x

Castanet, J., Francillon-Vieillot, H., Meunier, F. J., & de Ricqlès, A. J. (1993). Bone and individual aging. In B. K. Hall (Ed.), Bone (Vol. 7, pp. 245-283). CRC Press.

Castanet, J., & Naulleau, G. (1985). La squelettochronologie chez les reptiles. II. Résultats expérimentaux sur la signification des marques de croissance squelettiques chez les serpents. Remarques sur la croissance et la longévité de la vipère Aspic. Annales Des Sciences Naturelles-zoologie Et Biologie Animale, 7, 41-62.

Cerda, I. A., Chinsamy, A., Pal, D., Apaldetti, C., Otero, A., Powell, J. E., & Martinez, R. N. (2017). Novel insight into the origin of the growth dynamics of sauropod dinosaurs. PloS one, 2017(6), e0179707-e0179707. https://doi.org/10.1371/journal.pone.0179707

Crabtree, D. R. (1987). Angiosperms of the northern Rocky Mountains: Albian to Campanian (Cretaceous) megafossil floras. Annals of the Missouri Botanical Garden, 74(4), 707-747. https://doi.org/10.2307/2399448

Chinsamy, A. (1994). Dinosaur Bone Histology: Implications and Inferences. The Paleontological Society Special Publications, 7, 213-228. https://doi.org/10.1017/S2475262200009539

Cubo, J., Woodward, H., Wolff, E., & Horner, J. R. (2015). First reported cases of biomechanically adaptive bone modeling in non-avian dinosaurs. PloS one, 2015(7), e0131131-e0131131. https://doi.org/10.1371/journal.pone.0131131

Cullen, T. M., Zanno, L., Larson, D. W., Todd, E., Currie, P. J., & Evans, D. C. (2021). Anatomical, morphometric, and stratigraphic analyses of theropod biodiversity in the Upper Cretaceous (Campanian) Dinosaur Park Formation. Canadian journal of earth sciences, 58(9), 870-884. https://doi.org/10.1139/cjes-2020-0145

Day, L. M., & Jayne, B. C. (2007). Interspecific scaling of the morphology and posture of the limbs during the locomotion of cats (Felidae). Journal of experimental biology, 210(Pt 4), 642-654. https://doi.org/10.1242/jeb.02703

de Buffrénil, V., & Quilhac, A. (2021). Bone Tissue Types: A Brief Account of Currently Used Categories. In V. de Buffrénil, A. J. de Ricqlès, L. Zylberberg, & K. Padian (Eds.), Vertebrate Skeletal Histology and Paleohistology (1 ed., pp. 147-182). CRC Press. https://doi.org/https://doi.org/10.1201/9781351189590

de Buffrénil, V., Quilhac, A., & Castanet, J. (2021). Bone Tissue Types: A Brief Account of Currently Used Categories. In V. de Buffrénil, A. J. de Ricqlès, L. Zylberberg, & K. Padian (Eds.), Vertebrate Skeletal Histology and Paleohistology (1 ed., pp. 626-644). CRC Press. https://doi.org/https://doi.org/10.1201/9781351189590

Deeming, D. C., & Birchard, G. F. (2007). Allometry of egg and hatchling mass in birds and reptiles: roles of developmental maturity, eggshell structure and phylogeny. Journal of zoology (1987), 271(1), 78-87. https://doi.org/10.1111/j.1469-7998.2006.00219.x

D'Emic, M. D., O'Connor, P. M., Sombathy, R. S., Cerda, I., Pascucci, T. R., Varricchio, D., Pol, D., Dave, A., Coria, R. A., & Curry Rogers, K. A. (2023). Developmental strategies underlying gigantism and miniaturization in non-avialan theropod dinosaurs. Science (American Association for the Advancement of Science), 379(6634), 811.

Dial, K. P. (2003). Wing-Assisted Incline Running and the Evolution of Flight. Science (American Association for the Advancement of Science), 299(5605), 402-404. https://doi.org/10.1126/science.1078237

Dial, K. P., Jackson, B. E., & Segre, P. (2008). A fundamental avian wing-stroke provides a new perspective on the evolution of flight. Nature, 451(7181), 985-989. https://doi.org/10.1038/nature06517

Dial, K. P., Randall, R. J., & Dial, T. R. (2006). What Use Is Half a Wing in the Ecology and Evolution of Birds? Bioscience, 56(5), 437-445. https://doi.org/10.1641/0006 3568(2006)056[0437:WUIHAW]2.0.CO;2

Dodson, P. (1971). Sedimentology and taphonomy of the Oldman Formation (Campanian), Dinosaur Provincial Park, Alberta (Canada). Palaeogeography, palaeoclimatology, palaeoecology, 10(1), 21-74. https://doi.org/10.1016/0031-0182(71)90044-7

Doube, M., Yen, S. C. W., Kłosowski, M. M., Farke, A. A., Hutchinson, J. R., & Shefelbine, S. J. (2012). Whole-bone scaling of the avian pelvic limb. Journal of anatomy, 221(1), 21 29. https://doi.org/10.1111/j.1469-7580.2012.01514.x

Earls, K. D. (2000). Kinematics and mechanics of ground take-off in the starling Sturnis vulgaris and the quail Coturnix coturnix. Journal of experimental biology, 203(Pt 4), 725-739. https://doi.org/10.1242/jeb.203.4.725

Erickson, G. M. (2005). Assessing dinosaur growth patterns: a microscopic revolution. Trends in ecology & evolution (Amsterdam), 20(12), 677-684. https://doi.org/10.1016/j.tree.2005.08.012

Erickson, G. M., Makovicky, P. J., Currie, P. J., Norell, M. A., Yerby, S. A., & Brochu, C. A. (2004). Gigantism and comparative life-history parameters of tyrannosaurid dinosaurs. Nature, 430(7001), 772-775. https://doi.org/10.1038/nature02699

Erickson, G. M., Rogers, K. C., & Yerby, S. A. (2001). Dinosaurian growth patterns and rapid avian growth rates. Nature, 412(6845), 429-433. https://doi.org/10.1038/35086558

Erickson, G. M., & Tumanova, T. A. (2000). Growth curve of Psittacosaurus mongoliensis Osborn (Ceratopsia: Psittacosauridae) inferred from long bone histology. Zoological journal of the Linnean Society, 130(4), 551-566. https://doi.org/10.1006/zjls.2000.0243

Fowler, D. W., Woodward, H. N., Freedman, E. A., Larson, P. L., & Horner, J. R. (2011). Reanalysis of "Raptorex kriegsteini"; a juvenile tyrannosaurid dinosaur from Mongolia PloS one, 2011(6), e21376-e21376. https://doi.org/10.1371/journal.pone.0021376

Francillon-Vieillot, H., de Buffrénil, V., Castanet, J., Géraudie, J., Meunier, F. J., Sire, Y., Zylberberg, L., & de Ricqlès, A. J. (1989). Microstructure and Mineralization of Vertebrate Skeletal Tissues. In J. G. Carter (Ed.), Skeletal Biomineralization: Patterns, Processes and Evolutionary Trends (pp. 471-530). American Geophysical Union.

Grossi, B., Loncomilla, P., Canals, M., & Ruiz-Del-Solar, J. (2019). Are Cursorial Birds Good Kinematic Models of Non-Avian Theropods? International journal of morphology, 37(2), 620-625. https://doi.org/10.4067/S0717-95022019000200620

Heers, A. M., & Dial, K. P. (2012). From extant to extinct: locomotor ontogeny and the evolution of avian flight. Trends in ecology & evolution (Amsterdam), 27(5), 296-305. https://doi.org/10.1016/j.tree.2011.12.003

Jerzykiewicz, T., & Sweet, A. (1987). Semi-arid floodplain as a paleoenvironmental setting of the Upper Cretaceous dinosaurs. Occasional Papers of the Tyrrell Museum of Paleontology, 3, 120-124.

Jones, T. D., Farlow, J. O., Ruben, J. A., Henderson, D. M., & Hillenius, W. J. (2000). Cursoriality in bipedal archosaurs. Nature (London), 406(6797), 716-718. https://doi.org/10.1038/35021041

Krassilov, V. A. (1981). Changes of Mesozoic vegetation and the extinction of dinosaurs. Palaeogeography, palaeoclimatology, palaeoecology, 34(3-4), 207-224. https://doi.org/10.1016/0031-0182(81)90065-1

Lamas, L. P., Main, R. P., & Hutchinson, J. R. (2014). Ontogenetic scaling patterns and functional anatomy of the pelvic limb musculature in emus (Dromaius novaehollandiae). PeerJ (San Francisco, CA), 716, e716-e716. https://doi.org/10.7717/peerj.716

Larson, D. W., & Currie, P. J. (2013). Multivariate analyses of small theropod dinosaur teeth and implications for paleoecological turnover through time. PloS one, 2013(1), e54329 e54329. https://doi.org/10.1371/journal.pone.0054329

Lu, J., Currie, P. J., Xu, L., Zhang, X., Pu, H., & Jia, S. (2013). Chicken-sized oviraptorid dinosaurs from central China and their ontogenetic implications. Die Naturwissenschaften, 100(2), 165-175. https://doi.org/10.1007/s00114-012-1007-0

Makovicky, P. J., & Norell, M. A. (2004). Troodontidae. In D. B. Weishampel, P. Dodson, & H. Osmóska (Eds.), The Dinosauria (2 ed., pp. 184-195): University of California Press.

Muir, G. D., Gosline, J. M., & Steeves, J. D. (1996). Ontogeny of bipedal locomotion: walking and running in the chick. The Journal of physiology, 493(Pt 2), 589-601. https://doi.org/10.1113/jphysiol.1996.sp021406

Nacarino-Meneses, C., & Köhler, M. (2018). Limb bone histology records birth in mammals. PloS one, 13(6), e0198511-e0198511. https://doi.org/10.1371/journal.pone.0198511

Padian, K., & Lamm, E.-T. (2013). Bone histology of fossil tetrapods: advancing methods, analysis, and interpretation. University of California Press.

Persons, W. S., & Currie, P. J. (2016). An approach to scoring cursorial limb proportions in carnivorous dinosaurs and an attempt to account for allometry. Scientific reports, 6(19828), 19828-19828. https://doi.org/10.1038/srep19828

Phillips, M. J., Gibb, G. C., Crimp, E. A., & Penny, D. (2009). Tinamous and Moa Flock Together: Mitochondrial Genome Sequence Analysis Reveals Independent Losses of Flight among Ratites. Systematic Biology, 59(1), 90-107. https://doi.org/10.1093/sysbio/syp079

Ponton, F., Elżanowski, A., Castanet, J., Chinsamy, A., Margerie, E. D., Ricqlès, A. D., & Cubo, J. (2004). Variation of the Outer Circumferential Layer in the Limb Bones of Birds. Acta ornithologica, 39(2), 137-140. https://doi.org/10.3161/068.039.0210

Purwandana, D., Ariefiandy, A., Imansyah, M. J., Seno, A., Ciofi, C., Letnic, M., & Jessop, T. S. (2016). Ecological allometries and niche use dynamics across Komodo dragon ontogeny. Die Naturwissenschaften, 103(3-4), 27. https://doi.org/10.1007/s00114-016-1351-6

Ramezani, J., Beveridge, T. L., Rogers, R. R., Eberth, D. A., & Roberts, E. M. (2022). Calibrating the zenith of dinosaur diversity in the Campanian of the Western Interior Basin by CA-ID-TIMS U–Pb geochronology. Scientific reports, 12(1), 16026. https://doi.org/10.1038/s41598-022-19896-w

Russell, D. A. (1969). A new specimen of Stenonychosaurus from the Oldman Formation (Cretaceous) of Alberta. Canadian journal of earth sciences, 6(4), 595-612. https://doi.org/10.1139/e69-059

Suganya, G., Leela, V., Paramasivam, A., Richard Jagatheesan, P. (2017). Growth performance of emu chicks reared under intensive farming conditions. International Journal of Science, Environment, and Technology, 6(6), 3367-3371.

van der Reest, A. J., & Currie, P. J. (2017). Troodontids (Theropoda) from the Dinosaur Park Formation, Alberta, with a description of a unique new taxon; implications for deinonychosaur diversity in North America. Canadian journal of earth sciences, 54(9), 919-935. https://doi.org/10.1139/cjes-2017-0031

Varricchio, D. J. (1993). Bone microstructure of the Upper Cretaceous theropod dinosaur Troodon formosus. Journal of vertebrate paleontology, 13(1), 99-104. https://doi.org/10.1080/02724634.1993.10011490

Varricchio, D. J. (1995). Taphonomy of Jack's Birthday Site, a diverse dinosaur bonebed from the Upper Cretaceous Two Medicine Formation of Montana. Palaeogeography, palaeoclimatology, palaeoecology, 114(2-4), 297-323. https://doi.org/10.1016/0031 0182(94)00084-L

Varricchio, D. J. (1997). Troodontidae. In P. J. Currie & K. Padian (Eds.), The Encyclopedia of Dinosaurs (pp. 749-754). San Diego: Academic Press.

Varricchio, D. J., Jackson, F., Borkowski, J. J., & Horner, J. R. (1997). Nest and egg clutches of the dinosaur Troodon formosus and the evolution of avian reproductive traits. Nature (London), 385(6613), 247-250. https://doi.org/10.1038/385247a0

Varricchio, D. J., Moore, J. R., Erickson, G. M., Norell, M. A., Jackson, F. D., & Borkowski, J. J. (2008). Avian paternal care had dinosaur origin. Science (American Association for the Advancement of Science), 322(5909), 1826-1828. https://doi.org/10.1126/science.1163245

Varricchio, D. J., Jackson, F. D., Jackson, R. A., & Zelenitsky, D. K. (2013). Porosity and water vapor conductance of two Troodon formosus eggs; an assessment of incubation strategy in a maniraptoran dinosaur. Paleobiology, 39(2), 278-296. https://doi.org/10.1666/11042

Wolfe, J. A., & Upchurch, G. R. (1986). Vegetation, climatic and floral changes at the Cretaceous-Tertiary boundary. Nature (London), 324(6093), 148-152. https://doi.org/10.1038/324148a0

Zanno, L. E., Varricchio, D. J., O'Connor, P. M., Titus, A. L., & Knell, M. J. (2011). A new troodontid theropod, Talos sampsoni gen. et sp. nov., from the Upper Cretaceous Western Interior Basin of North America. PloS one, 2011(9), e24487. https://doi.org/10.1371/journal.pone.0024487

Zhang, F., Zhou, Z., Xu, X., & Wang, X. (2002). A juvenile coelurosaurian theropod from China indicates arboreal habits. Die Naturwissenschaften, 89(9), 394-398. https://doi.org/10.1007/s00114-002-0353-8

APPENDICES

APPENDIX A

TROODON MEASUREMENTS AND ANNUAL GROWTH RATES

Specimen No.	Field No.	Femur Length (mm)	Femur Minimal Circumference (mm)	Tibia Length (w/o astragalus)	Tibia Shaft Least Circumference (mm)	MTII Length (mm)	MTIII Length (mm)	MT IV Length (mm)	Body Mass based on Campione et al 2014 (kg)	Body Mass Based on D'Emic et al 2023 (kg)
MOR 748	7.26.93	320	86	350	80	180	214	211	44.12	40.56
MOR 553s	7.28.91.239	284	87						45.54	
MOR 553s	7.29.92.113									
MOR 553s	8.7.9.417	235	63						18.72	
MOR 553s	7.16.0.61	330	103						72.50	
MOR 553s	7.28.91.234	221	66						21.28	
MOR 553s	7.22.91.164	240	67						22.18	
MOR 553	11.1.01.1									
MOR 553s	7.11.91.41			374	83					45.20
MOR 553s	7.8.91.28									
MOR 553s	11.1.01.8					*209*	*248.5*	245		
MOR 553s	8.16.92.254			365	87					51.92
MOR 553s	7.17.0.74			317	68					25.15
MOR 553s	8.17.92.260						*200.8*	198		
MOR 553	7.8.91.28					142	*168.8*	*166.5*		
MOR 553	7.18.92.5					202	*240.2*	*236.8*		
MOR 553s	7.28.91.237				98					73.76
MOR 553E	N/A			317	68					25.15
MOR 553E	7.1.9.9					*122.0*	*145.0*	143		
MOR 553s	7.20.91.132			278	58					15.77
MOR 553L	7.28.8.102					*214.1*	*254.6*	251		
MOR 553L	7.24.8.64			430	95					67.30
MOR 430	5.20.86	126	37.5	*160*	30				4.49	2.31
MOR 563			56		58				13.54	15.77
MOR 246-11		35	11	46		*33.3*	*39.6*	39	0.22	

**Italicized measurements are estimates.*

TABLE A.1. Full list of *Troodon* bone measurements and associated body mass estimates.

Museum ID	Field No.	Proj. No.	Slide/ Bone No.	Full Bone Circ. (mm)	Histo. Sample circ. (mm)	Circ. Variation Quotient	Full individual Body Mass (kg)
MOR 430	5.20.86	2002-08C	T1	30	32	0.94	2.31
MOR 553S	7.11.91.41	2003-23C	T1-4	83	88	0.94	45.20
MOR 553L	7.24.8.64	2003-23C	T2-2	95	101	0.94	67.30
MOR 553S	7.28.91.23	2003-23C	T3-1	98	105	0.93	73.76
MOR 553S	7.28.91.23	2003-23C	T3-2	98	106	0.92	73.76
MOR 553S	7.28.91.23	2003-23C	T3-3	98	104	0.94	73.76
MOR 553S	7.28.91.23	2003-23C	T3-4	98	104	0.94	73.76
MOR 553S	7.28.91.23	2003-23C	T3-5	98	103	0.95	73.76
MOR 553S	7.17.0.74	1992-03	T5	68	68	1.00	25.15
MOR 553S	7.20.91.13	1992-03	T6	58	61	0.95	15.77
MOR 563	7.27.88.1	1991-08	T2-1	58	64	0.91	15.77
MOR 748	7.26.93	2002-08C	T2-1	80	84	0.95	40.56
MOR 748	7.26.93	2002-08C	T2-2	80	85	0.94	40.56
MOR 748	7.26.93	2002-08C	T2-4	80	87	0.92	40.56
MOR 748	7.26.93	1996-15	F-2	86	96	0.90	44.12

TABLE A.2. Full circumferences of bones observed in histological slides and corresponding body masses.

Museum ID	Field No.	Proj. No.	SGM 1 circ. (mm)	Body Mass (kg)	SGM 2 circ. (mm	Body Mass (kg)	SGM 3 circ. (mm	Body Mass (kg)	SGM 4 circ. (mm	Body Mass (kg)	SGM 5 circ. (mm	Body Mass (kg)	SGM 6 circ. (mm	Body Mass (kg)	SGM 7 circ. (mm	Body Mass (kg)	SGM 8 circ. (mm)	Body Mass (kg)	SGM 9 circ. (mm	Body Mass (kg)	SGM 10 circ. (mm)	Body Mass (kg)	SGM 11 circ. (mm)	Body Mass (kg)	SGM 12 circ. (mm)	Body Mass (kg)
MOR 430	5.20.86	2002-08C																								
MOR 553S	7.11.91.41	2003-23C	55	11.4	*65*	*18.6*	*74*	*27.2*	81	35.4	*83*	*38.1*	86	42.2	87	43.7										
MOR 553L	7.24.8.64	2003-23C	86	41.9	88	44.8	91	49.5	96	57.9	98	61.6	101	67.3												
MOR 553S	7.28.91.23	2003-23C	71	23.3	73	25.3	89	45.3	97	58.4	102	67.7	105	73.8												
MOR 553S	7.28.91.23	2003-23C	68	20.0	73	24.6	88	42.6	96	55.1	102	65.8	105	71.7												
MOR 553S	7.28.91.23	2003-23C	68	21.1	72	25.0	87	43.6	97	60.1	102	69.7	104	73.8												
MOR 553S	7.28.91.23	2003-23C	66	19.4	70	23.0	87	43.6	95	56.5	101	67.7	104	73.8												
MOR 553S	7.28.91.23	2003-23C	68	21.7	73	26.8	88	46.4	95	58.1	99	65.6	103	73.8												
MOR 553S	7.17.0.74	1992-03	65	22.0																						
MOR 553S	7.20.91.13	1992-03	48	7.8	55	11.6																				
MOR 563	7.27.88.1	1991-08	*54*	*9.6*																						
MOR 748	7.26.93	2002-08C	46	6.9	58	13.7	66	20.0	73	26.8	77	31.4	79	33.9	81	36.4	83	39.2	84	40.6						
MOR 748	7.26.93	2002-08C	46	6.7	*51*	*9.1*	59	13.9	67	20.2	73	25.9	*78*	*31.5*	*80*	*33.9*	81	35.2	83	37.8	*84*	*39.2*	84.5	39.9	85	40.6
MOR 748	7.26.93	2002-08C	46	6.3	*51*	*8.5*	59	13.0	*63*	*15.7*	68	19.7	73	24.2	77	28.3	79	30.5	81	32.9	85	37.9	88	41.9		
MOR 748	7.26.93	1996-15	*56*	*10.0*	64	14.4	*66*	*15.7*	*69*	*17.8*	73	20.8	80	26.7	87	33.6	89	35.8	91	38.1	93	40.4	94	41.6	96	44.1

**Italicized values indicate annuli*

TABLE A.3. Circumferences of SGMs observed in histologic thin sections and their corresponding body masses.

APPENDIX B

DROMAIUS HIND LIMB MEASUREMENTS

Specimen No.	Age (days)	Femur Length (mm)	Femur Circ. (mm)	Tibia Length (mm)	Tarsometatarsus Length (mm)	Estimated Body Mass (Anderson et al., 1985) (kg)
VP-0938B		210	90	340	300	30.8
VP-0938C		227	90			30.8
HRB-001		36	14	60	51	0.4
HRB-002		94	41	140	129	5.1
HRB-003	*248*	220	98	383	350	37.4
HRB-004		70	29	109	85	2.3
HRB-005		71	31	108	95	2.7
HRB-006	19	53	20	89	75	1.0
HRB-007		64	30	100	95	2.5
HRB-008	14	40	15	68	54	0.5
HRB-009		60	21	91	78	1.1
HRB-010	60	97	43	154	130	5.7
HRB-011		45	20	76	65	1.0
HRB-012	28	70	31	105	91	2.7
HRB-013		61	24	95	82	1.5
HRB-014		135	58	220	200	11.3
HRB-015		152	59	242	230	11.8
HRB-016		130	57	212	197	10.9
HRB-017	84	146	59	236	219	11.8
HRB-018		158	59	255	242	11.8
HRB-019		170	62	285	261	13.2
HRB-020	99	140	55	230	208	10.0
HRB-021	130	178	69	290	270	16.8
HRB-022		183	71	288	273	18.0
HRB-023		185	83	325	313	25.6
HRB-025	141	180	65	295	276	14.7
HRB-026		163	60	280	270	12.2
HRB-027		183	69	300	283	16.8
HRB-028	142	178	79	296	283	22.9
HRB-031		127	54	210	181	9.6
HRB-032		81	39	134	115	4.6
HRB-034		186	74	307	295	19.7
HRB-035		181	69	301	275	16.8
HRB-036		210	92	345	325	32.4
HRB-037		183	65	305	280	14.7

TABLE A.4. Basic emu hind limb bone measurements and their corresponding body masses.

APPENDIX C

WITHIN-ELEMENT PROPORTIONAL MEASUREMENTS OF *TROODON* AND *DROMAIUS* HIND LIMB BONES

Specimen No.	Taxon	Field No.	Age (days)	Element	Max. Proximal A/P (mm)	Max. Proximal M/L (mm)	Shaft A/P Diameter (mm)	Shaft M/L Diameter (mm)	Max Distal A/P (mm)	Max Distal M/L (mm)
MOR 748	Troodon	7.26.93		femur	57	60	27	28	47	53
MOR 553	Troodon	7.28.91.239		femur	49	64	28	29	42	56
MOR 553	Troodon	8.7.9.417		femur	30	35	20	18	N/A	N/A
MOR 553	Troodon	7.22.91.164		femur	33	43	19	20	26	40
MOR 553	Troodon	7.16.0.61		femur	N/A	49	19	19	36	46
MOR 553	Troodon	7.28.91.234		femur	N/A	70	31	32	63	71
HRB-001	Emu			femur	9	7	4	4	8	9
HRB-002	Emu			femur	23	21	13	12	25	25
HRB-003	Emu		*248*	femur	57	54	30	28	62	70
HRB-004	Emu			femur	16	15	9	8	15	18
HRB-005	Emu			femur	17	15	8	10	18	19
HRB-006	Emu		19	femur	12	11	5	6	12	14
HRB-007	Emu			femur	16	14	8	9	15	17
HRB-008	Emu		14	femur	10	8	4	4	9	10
HRB-009	Emu			femur	12	10	6	6	14	15
HRB-010	Emu		60	femur	23	21	12	12	24	26
HRB-011	Emu			femur	11	9	6	5	11	11
HRB-012	Emu		28	femur	17	16	8	9	18	18
HRB-013	Emu			femur	14	11	6	7	14	14
HRB-014	Emu			femur	35	33	15	19	39	42
HRB-015	Emu			femur	37	34	19	17	41	44
HRB-016	Emu			femur	34	30	19	16	37	38
HRB-017	Emu		84	femur	35	32	15	19	39	41
HRB-018	Emu			femur	36	35	18	18	42	45
HRB-019	Emu			femur	40	37	21	16	42	49
HRB-020	Emu		99	femur	35	31	17	16	38	40
HRB-021	Emu		130	femur	40	42	21	22	45	50
HRB-023	Emu			femur	47	44	26	27	53	57
HRB-025	Emu		141	femur	41	40	17	22	49	52
HRB-026	Emu			femur	39	38	18	20	45	49
HRB-027	Emu			femur	45	39	22	21	50	49
HRB-028	Emu		142	femur	45	43	22	27	51	56
HRB-031	Emu			femur	32	29	17	16	35	37
HRB-032	Emu			femur	19	18	12	13	20	24
HRB-034	Emu			femur	46	42	24	21	51	54
HRB-035	Emu			femur	44	38	23	19	49	49
HRB-036	Emu			femur	40	62	26	32	59	59
HRB-037	Emu			femur	44	38	22	18	47	52

TABLE A.5. *Troodon* and emu femoral dimensions.

Specimen No.	Taxon	Field No.	Age (days)	Element	Max. Proximal A/P (mm)	Max. Proximal M/L (mm)	Shaft A/P Diameter (mm)	Shaft M/L Diameter (mm)	Max Distal A/P (mm)	Max Distal M/L (mm)	Shaft min. circ. (mm)	Distal epiphysis circ. (mm)
MOR 748	Troodon	7.26.93		tibia	56	44	25	27	20	49	80	110
MOR 553	Troodon	7.11.91.41		tibia	77	44	23	30	17	57	83	105
MOR 553	Troodon	8.16.92.254		tibia	61	52	24	28	18	57	87	110
MOR 553	Troodon	7.17.0.74		tibia	57	25	19	23	15	44	68	100
MOR 553	Troodon	N/A		tibia	43	N/A	19	23	N/A	N/A	68	100
MOR 553	Troodon	7.20.91.132		tibia	22	N/A	17	20	15	41	58	80
MOR 553	Troodon	7.24.8.64		tibia	64	53	N/A	33	19	63	95	115
MOR 430	Troodon	5.20.86		tibia	N/A	N/A	9	10	8	16	30	
HRB-001	Emu			tibiotarsus	11	6	3	3	4	10	6	
HRB-002	Emu			tibiotarsus	34	19	9	9	11	25	17	
HRB-003	Emu		*248*	tibiotarsus	78	50	22	26	21	46	40	
HRB-004	Emu			tibiotarsus	24	14	6	7	8		13	
HRB-005	Emu			tibiotarsus	23	14	7	9	8	19	13	
HRB-006	Emu		19	tibiotarsus	17	9	5	5	4	14	8	
HRB-007	Emu			tibiotarsus	21	13	7	7	7	18	10	
HRB-008	Emu		14	tibiotarsus	13	7	3	3	5	11	7	
HRB-009	Emu			tibiotarsus	18	11	5	6	7	15	9	
HRB-010	Emu		60	tibiotarsus	34	19	12	11	11	25	17	
HRB-011	Emu			tibiotarsus	15	8	4	5	6	13	9	
HRB-012	Emu		28	tibiotarsus	14	24	9	9	9	20	13	
HRB-013	Emu			tibiotarsus	20	12	5	5	7	16	11	
HRB-014	Emu			tibiotarsus	48	28	13	17	18	37	26	
HRB-015	Emu			tibiotarsus	54	30	14	15	17	37	27	
HRB-016	Emu			tibiotarsus	46	26	13	13	15	35	25	
HRB-017	Emu		84	tibiotarsus	51	28	14	15	16	36	25	
HRB-018	Emu			tibiotarsus	54	33	15	17	19	38	28	
HRB-019	Emu			tibiotarsus	58	33	19	16	18	40	29	
HRB-020	Emu		99	tibiotarsus	49	28	15	14	15	36	25	
HRB-021	Emu		130	tibiotarsus	61	34	18	19	18	41	30	
HRB-023	Emu			tibiotarsus	71	40	22	25	14	41	37	
HRB-025	Emu		141	tibiotarsus	63	38	22	19	21	41	32	
HRB-026	Emu			tibiotarsus	61	35	15	16	19	42	29	
HRB-027	Emu			tibiotarsus	63	35	20	19	19	42	32	
HRB-028	Emu		142	tibiotarsus	67	37	21	21	23	45	32	
HRB-031	Emu			tibiotarsus	45	26	14	15	17	34	24	
HRB-032	Emu			tibiotarsus	28	17	9	10	11	23	16	
HRB-034	Emu			tibiotarsus	65	38	18	21	23	45	35	
HRB-035	Emu			tibiotarsus	58	35	17	20	21	44	31	
HRB-036	Emu			tibiotarsus	77	43	27	27	19	46	38	
HRB-037	Emu			tibiotarsus	63	37	17	19	19	43	32	

TABLE A.6. *Troodon* and emu tibial dimensions

Specimen No.	Taxon	Field No.	Element	Max. Proximal A/P (mm)	Max. Proximal M/L (mm)	Shaft A/P Diameter (mm)	Shaft M/L Diameter (mm)	Max Distal A/P (mm)	Max Distal M/L (mm)	Shaft Circ. (mm)
MOR 430	Troodon	5.20.86	MTIII	N/A	N/A	N/A	N/A			
MOR 553s	Troodon	7.16.91.79	MTIII	N/A	N/A	N/A	N/A	25	22	
MOR 553s	Troodon	7.29.92.113	MTIII	N/A	N/A	N/A	N/A	21	16	
MOR 553s	Troodon	8.6.9.406	MTIII	N/A	N/A	N/A	N/A	21	18	
MOR 748	Troodon	7.26.93	MTIII	N/A	N/A	N/A	N/A	25	20	
MOR 553	Troodon	11.1.01.8	MTIV	42	38	21-25	21-24	33	25	55
MOR 553	Troodon	8.17.92.260	MTIV	36	28	14-19	15-16	21	16	40
MOR 553	Troodon	7.1.9.9	MTIV	20	N/A	9-14	9-11	15	10	23
MOR 553	Troodon	7.28.8.102	MTIV	N/A	38	22-25	19-23	28	23	55
MOR 748	Troodon	7.26.93	MTIV	31	30	16-24	14-18	23	19	40

TABLE A.7. *Troodon* metatarsal dimensions.

Specimen No.	Taxon	Age (days)	Element	Max. Proximal A/P (mm)	Max. Proximal M/L (mm)	Shaft A/P Diameter Range (mm)	Shaft A/P Midshaft Diameter (mm)	Shaft M/L Diameter Range (mm)	Shaft M/L Midshaft Diameter (mm)	Max Distal A/P (mm)	Max Distal M/L (mm)	MTIII A/P (mm)	MTIII M/L (mm)	MTII Length (mm)	MTIII Length (mm)	MTIV Length (mm)
HRB-001	Emu		tmt	7	10	2-5	3	4-7	4	5	10	4	5	48	51	49
HRB-002	Emu		tmt	18	24	6-15	8	9-20	10	14	25	12	14	123	129	125
HRB-003	Emu	*248*	tmt	41	50	13-28	19	18-35	22	30	49	24	26	337	350	343
HRB-004	Emu		tmt	11	18	4-9	5	6-12	7	9	17	7	9	80	85	82
HRB-005	Emu		tmt	14	21	4-9	5	6-13	7	11	19	8	10	92	95	93
HRB-006	Emu	19	tmt	10	14	3-7	4	5-10	6	8	13	5	7	71	75	73
HRB-007	Emu		tmt	13	20	4-10	5	6-12	7	9	18	8	10	89	95	92
HRB-008	Emu	14	tmt	7	11	2-5	3	4-8	4	6	11	5	5	51	54	52
HRB-009	Emu		tmt	11	16	3-10	4	4-14	5	8	14	6	8	74	78	75
HRB-010	Emu	60	tmt	19	27	7-16	9	7-20	11	15	23	11	13	126	130	128
HRB-011	Emu		tmt	9	12	3-7	4	5-9	5	8	12	6	6	61	65	62
HRB-012	Emu	28	tmt	14	19	4-9	5	7-11	7	11	18	9	9	86	91	88
HRB-013	Emu		tmt	12	16	3-9	4	5-11	5	9	16	7	8	79	82	80
HRB-014	Emu		tmt	27	39	8-20	12	12-24	13	21	34	16	17	192	200	196
HRB-015	Emu		tmt	30	41	9-21	13	11-27	14	22	35	18	18	220	230	223
HRB-016	Emu		tmt	27	38	7-20	11	11-27	13	19	30	14	17	188	197	190
HRB-017	Emu	84	tmt	28	37	9-20	11	11-27	13	20	34	16	19	210	219	214
HRB-018	Emu		tmt	29	42	7-20	13	12-26	14	23	39	17	18	233	242	236
HRB-019	Emu		tmt	32	43	9-21	13	12-28	14	25	34	17	20	245	261	250
HRB-020	Emu	99	tmt	26	38	8-19	11	10-26	12	19	31	15	17	193	208	197
HRB-021	Emu	130	tmt	33	44	10-21	15	12-27	15	23	38	18	21	262	270	265
HRB-023	Emu		tmt	37	47	11-22	16	14-27	18	23	43	21	22	297	313	306
HRB-025	Emu	141	tmt	37	45	11-22	16	15-32	16	23	42	20	24	264	276	269
HRB-026	Emu		tmt	31	43	8-19	13	12-27	14	22	39	17	20	253	270	257
HRB-027	Emu		tmt	34	46	11-21	15	15-29	18	23	42	19	22	272	283	275
HRB-028	Emu	142	tmt	38	49	10-28	16	15-33	18	24	41	19	23	274	283	278
HRB-031	Emu		tmt	25	37	7-19	10	11-28	13	19	31	15	18	169	181	171
HRB-032	Emu		tmt	16	22	5-12	6	8-15	9	12	22	9	12	107	115	111
HRB-034	Emu		tmt	35	48	10-25	16	14-32	17	25	43	19	24	283	295	285
HRB-035	Emu		tmt	31	45	10-20	14	13-28	15	27	40	19	20	265	275	268
HRB-036	Emu		tmt	27	48	18	18	17-33	21	30	46	21	26	304	325	307
HRB-037	Emu		tmt	36	48	10-26	16	15-34	17	24	38	18	21	262	280	270

TABLE A.8. Emu tarsometatarsal dimensions

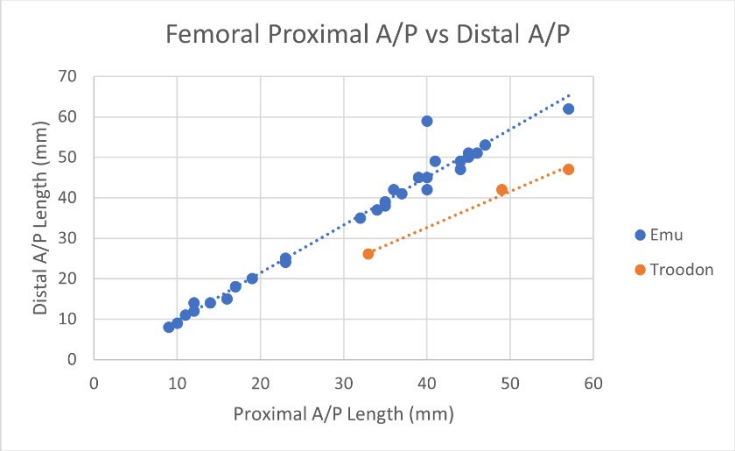

FIGURE A.1. Emu and *Troodon* femur proximal vs. distal anteroposterior dimensions.

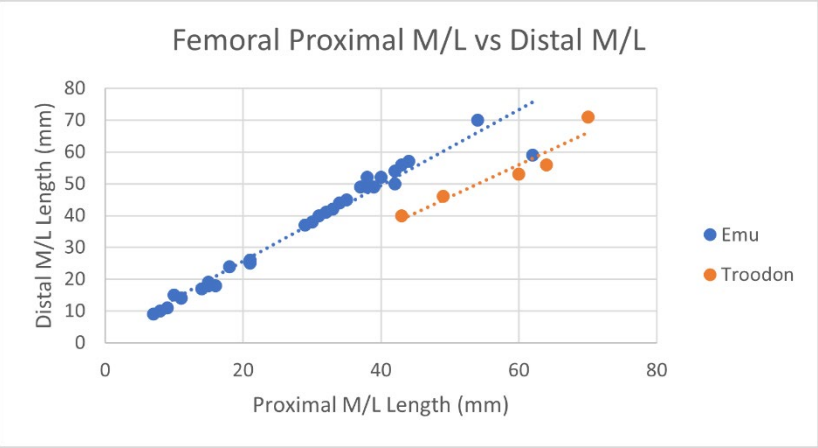

FIGURE A.2. Emu and *Troodon* femur proximal vs. distal mediolateral dimensions.

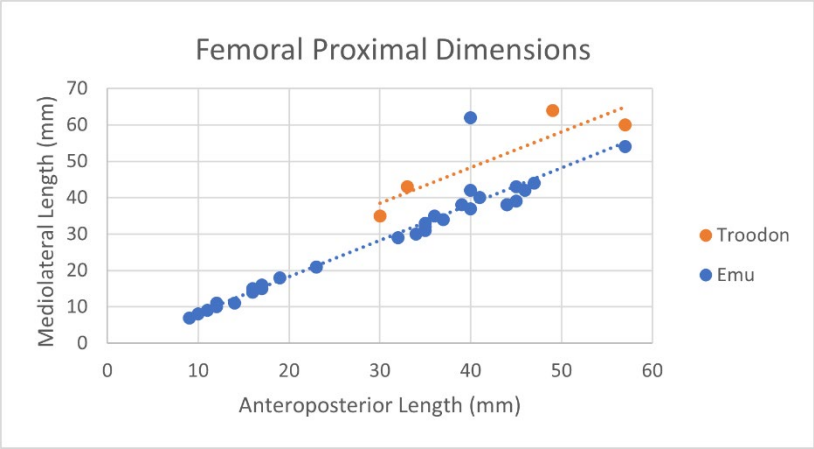

FIGURE A.3. Emu and *Troodon* femur proximal dimensions.

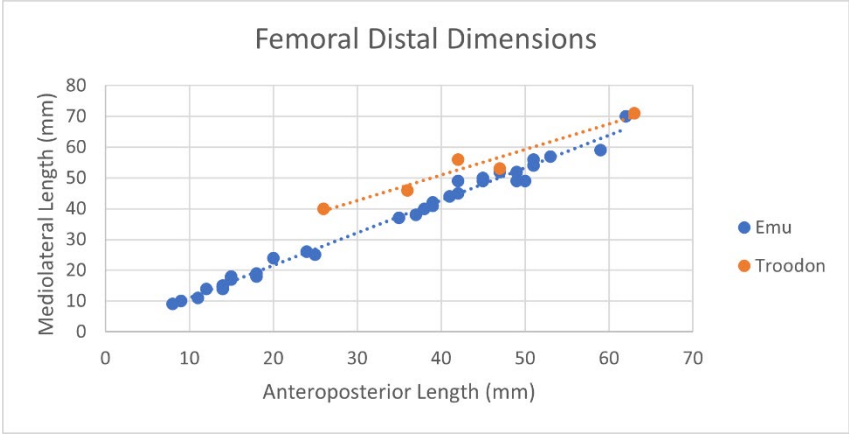

FIGURE A.4. Emu and *Troodon* femur distal dimensions.

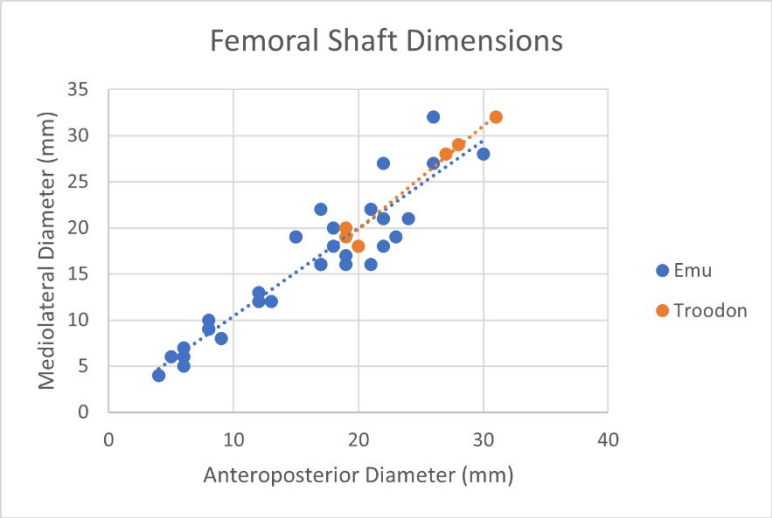

FIGURE A.5. *Troodon* and emu femoral shaft dimensions.

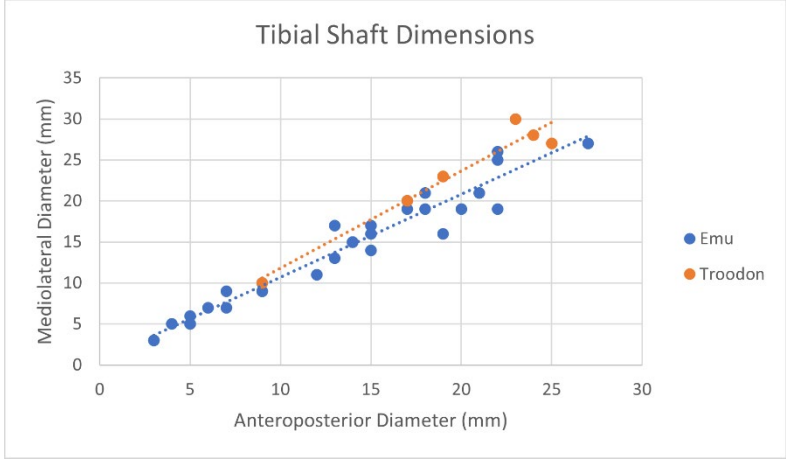

FIGURE A.6. *Troodon* and emu tibial shaft dimensions.

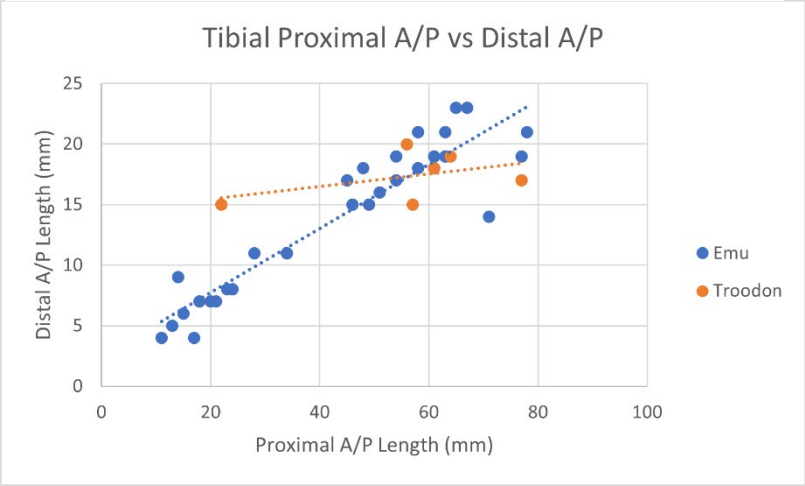

FIGURE A.7. Emu and *Troodon* tibia proximal vs. distal anteroposterior dimensions.

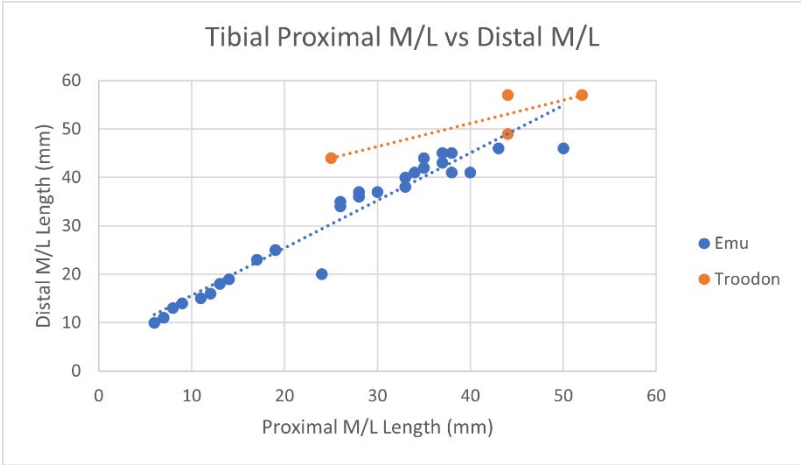

FIGURE A.8. Emu and *Troodon* tibia proximal vs. distal mediolateral dimensions.

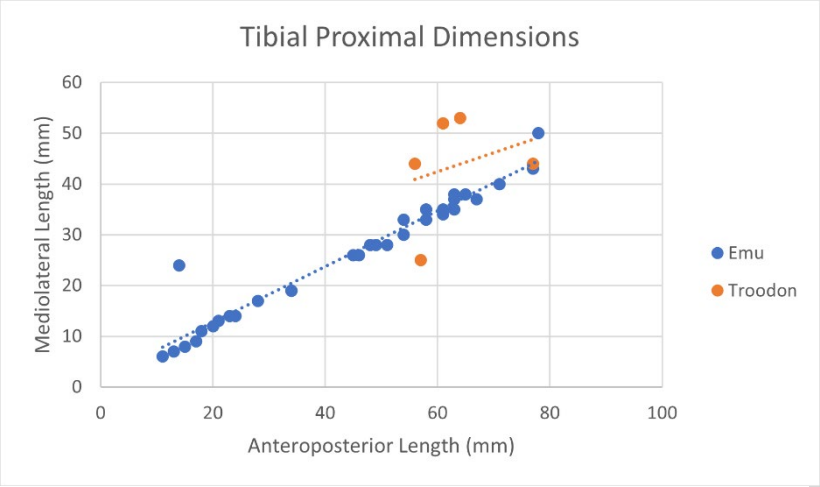

FIGURE A.9. *Troodon* and emu tibial proximal dimensions

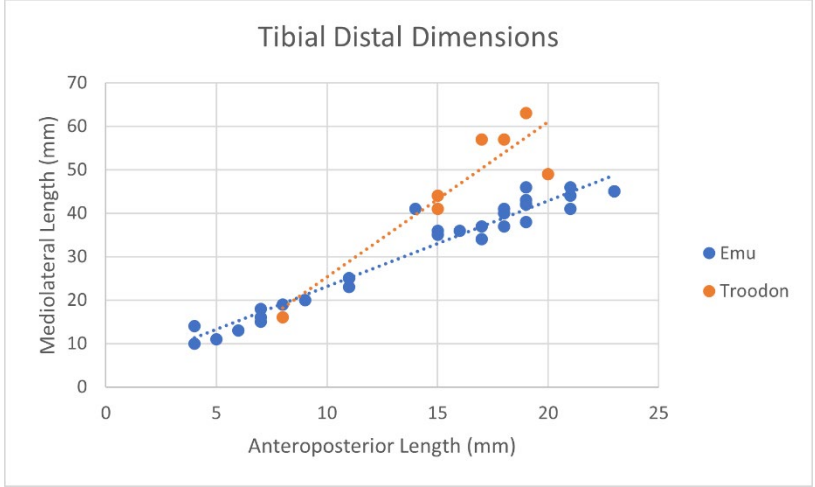

FIGURE A.10. *Troodon* and emu tibial distal dimensions.

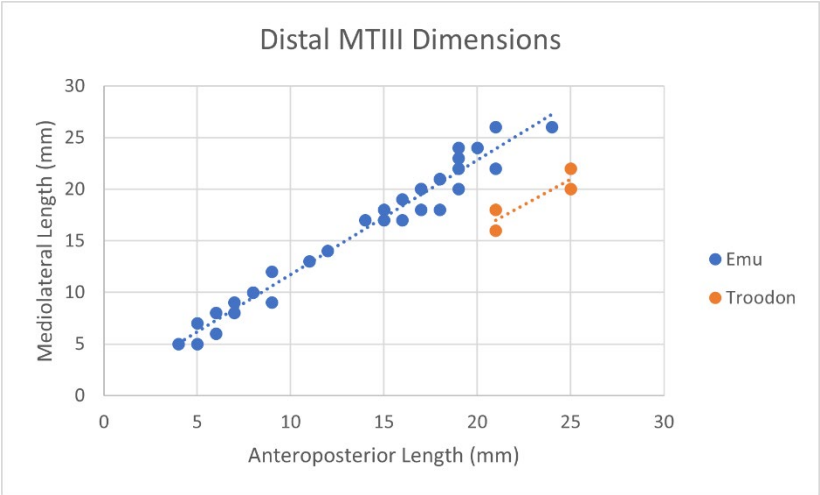

FIGURE A.11. *Troodon* and emu distal third metatarsal dimensions.

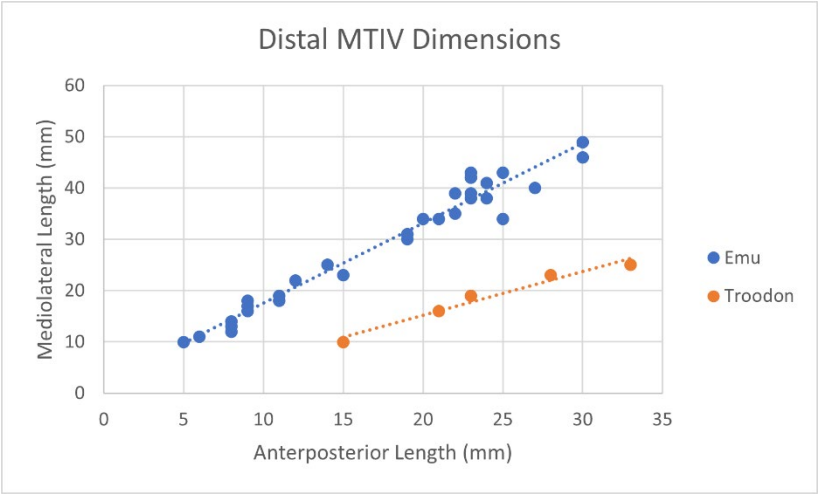

FIGURE A.12. *Troodon* and emu distal fourth metatarsal dimensions.